

# Microstructural and Mechanical Properties Characterization of Wire Arc Additive Manufacturing with GMAW for 308 Stainless Steel



UNIVERSITI TEKNIKAL MALAYSIA MELAKA

2024



**MICROSTRUCTURE AND MECHANICAL PROPERTIES  
CHARACTERIZATION OF WIRE ARC ADDITIVE  
MANUFACTURING FOR 308 STAINLESS STEEL**

This report is submitted in accordance with requirement of the University Teknikal Malaysia Melaka (UTeM) for Bachelor Degree of Manufacturing Engineering (Hons.)

اونيورسي تيكنيكل مليسيا ملاك  
UNIVERSITI TEKNIKAL MALAYSIA MELAKA

by

**MUHAMAD FAKHRUR RAZI BIN ALAMI**

FACULTY OF INDUSTRIAL AND MANUFACTURING  
TECHNOLOGY AND ENGINEERING

2024

## DECLARATION

I hereby, declared this report entitled “Microstructure and Mechanical Properties Characterization of Wire Arc Additive Manufacturing with GMAW for 308 Stainless Steel” is the result of my own research except as cited in references.

Signature : .....

Author's Name : MUHAMAD FAKHRUR RAZI BIN ALAMI

Date : 26 JUNE 2024

UNIVERSITI TEKNIKAL MALAYSIA MELAKA



## ABSTRAK

Penyelidikan ini memberi tumpuan kepada pencirian mikrostruktur dan sifat mekanikal keluli tahan karat 308 yang dihasilkan melalui Wire Arc Additive Manufacturing (WAAM) menggunakan Gas Metal Arc Welding (GMAW). Kajian ini menggunakan sistem EWM GMAW yang dikawal oleh robot KUKA untuk penyediaan sampel, dengan Reka Bentuk Eksperimen (DoE) berdasarkan kaedah Taguchi, yang menggabungkan pemboleh ubah seperti arus kimpalan, voltan, dan kelajuan. Objektif kajian adalah untuk menyiasat hubungan antara parameter proses ini dengan mikrostruktur dan sifat mekanikal bahan yang didepositkan. Pencirian bahan dilakukan menggunakan Mikroskopi Elektron Imbasan (SEM), sementara ujian tegangan dan kekerasan, yang mematuhi piawaian ASTM E8/E8M, menilai sifat mekanikal. Penemuan menunjukkan kepentingan pengoptimuman proses dalam meningkatkan prestasi dan kebolehpercayaan komponen keluli tahan karat 308, menjadikan hasil kajian ini bernilai untuk aplikasi industri, khususnya dalam sektor penjaan kuasa. Kajian ini menyumbang kepada pemahaman tentang kesan parameter proses WAAM pada keluli tahan karat 308, memberikan pandangan untuk mengoptimumkan proses pembuatan bagi mencapai sifat bahan yang diinginkan.

## **ABSTRACT**

This research is focused on characterizing the microstructure and mechanical properties of 308 stainless steel fabricated by Wire Arc Additive Manufacturing using Gas Metal Arc Welding. The samples produced in this research were deposited using an EWM GMAW system controlled by a KUKA robot, while the design of the experiment was carried out using the Taguchi method, which consisted of variables including welding current, voltage, and speed. This work seeks to relate such process parameters to the resulting microstructure and mechanical properties of the deposited material. Material characterization was carried out using SEM, while tensile and hardness tests, following ASTM E8/E8M standards, evaluated mechanical properties. The findings demonstrate that process optimization has huge potential in the real improvement of performance and reliability of 308 stainless steel components; hence, it has significantly high value in industrial applications, especially within the sector of power generation. This research will help add to the current literature an understanding of how WAAM process parameters influence 308 SS candidates, thus allowing some valuable insights related to the optimization of manufacturing processes with respect to the properties required of the materials.

## DEDICATION

This dedication is a heartfelt expression of gratitude for my parent, Alami Bin Rasit and Suhaila Binti Ayub, for the lessons learned in times of adversity and the immeasurable love that has been the foundation of my being. Thank you for being my constant source of strength and inspiration.

To my supervisor, Associate Professor Dr Nur Izan Binti Hussien, this dedication is a tribute to your unwavering belief in my potential, your invaluable guidance that has illuminated my path, and your patience that has allowed me to flourish. I am grateful for the opportunities that have been provided and the knowledge that has been shared.

To all my friends, I appreciate the countless memories we've created, the support you've offered without hesitation, and the understanding that defines our bond.

## ACKNOWLEDGEMENT

I am grateful to my supervisor, Associate Professor Dr Nur Izan Syahriah Binti Hussein, for her support and guidance in completing this project research successfully. Thank you for all your guidance, encouragement, advice, and opportunities for me to learn. Endure the experience while working on the Final Year Project.

Finally, I want to appreciate and thank my parents and family for their encouragement and supporting me in completing this project successfully. I want to thank my pals for their encouragement and help overcoming challenges during this endeavour.

UNIVERSITI TEKNIKAL MALAYSIA MELAKA

# TABLE OF CONTENT

ABSTRAK.....	i
ABSTRACT.....	ii
DEDICATION .....	iii
ACKNOWLEDGEMENT .....	iv
TABLE OF CONTENT .....	v
LIST OF FIGURES .....	ix
LIST OF ABBREVIATIONS .....	xi
LIST OF SYMBOLS .....	xii
<b>CHAPTER 1 INTRODUCTION.....</b>	<b>1</b>
1.1 Background of study.....	1
1.2 Problem statement.....	2
1.3 Objectives .....	3
1.4 Scope of study.....	4
1.5 Significance of study.....	4
1.6 Research planning.....	5
<b>CHAPTER 2 LITERATURE REVIEW .....</b>	<b>6</b>
1.1 Introduction.....	6
2.1 Wire arc additive manufacturing (WAAM) .....	6
2.2 WAAM applications.....	9
2.3 Material characteristics .....	10
2.3.1 308 Stainless Steel .....	10
2.4 Microstructural properties of wire arc additive Manufacturing (WAAM) .....	11

2.4.1	Grain Structure.....	13
2.4.2	Crack.....	16
2.4.3	Porosity.....	17
2.5	Mechanical properties characterization.....	19
2.5.1	Tensile Strength.....	20
2.5.2	Microhardness.....	21
2.6	Process parameters of wire arc additive manufacturing.....	22
2.6.1	Heat input.....	23
2.6.2	Welding speed.....	24
2.7	Effect of process parameters on bead quality.....	24
2.8	Defect analysis.....	25
<b>CHAPTER 3 METHODOLOGY.....</b>		<b>27</b>
3.1	Introduction.....	27
3.2	Gantt chart.....	28
3.3	Flow chart.....	29
3.4	Material Preparation.....	29
3.4.1	308 stainless steel wire.....	29
3.5	Design of Experiment (DoE).....	30
3.5.1	Taguchi Method.....	31
3.6	WAAM Process.....	32
3.7	Experiment Method.....	33
3.7.1	Analysis of the deposition geometry.....	34
3.7.2	Microstructure (SEM).....	34
3.7.3	Tensile Testing.....	35
<b>CHAPTER 4 RESULT AND DISCUSSION.....</b>		<b>37</b>
4.1	Introduction.....	37

4.2	Preliminary Experiment .....	37
4.3	Design Matrix .....	43
4.4	Relationship parameters and response .....	44
4.5	Microstructural analysis .....	45
4.6	Fracture surface analysis .....	47
4.7	Tensile Properties .....	49
4.8	Effect of parameter on bead dimension .....	50
4.8.1	Analysis between parameter and width .....	50
4.8.2	Analysis between parameter and height .....	51
4.9	Optimization of parameter .....	52
4.10	Regression model .....	55
4.11	Summary .....	56
<b>CHAPTER 5 CONCLUSION AND RECOMENDATION .....</b>		<b>57</b>
5.1	Conclusion .....	57
5.2	Sustainable development .....	58
5.3	Complexity .....	58
5.4	Lifelong learning .....	59
5.5	Recommendations .....	60
<b>REFERENCES .....</b>		<b>61</b>
<b>APPENDIX A .....</b>		<b>66</b>
Gantt chart of PSM 1 .....		66
Gannt Chart PSM 2 .....		67

## LIST OF TABLES

Table 2.1: Tensile properties of GMAW-AM 316 L and wrought 316 L. (Vora et al., 2022)	20
Table 3.1: Gantt Chart	28
Table 3.2: Chemical composition of 308 Stainless steel	30
Table 3.3: Variable for process parameters	31
Table 3.4: Design of Experiment	32
Table 4.1 Design of Experiment using Taguchi method	38
Table 4.2 Design matrix	44
Table 4.3 Mechanical properties data	49
Table 4.4 Optimization value for width effect	53
Table 4.5 Optimization value for height effect	54

UNIVERSITI TEKNIKAL MALAYSIA MELAKA

## LIST OF FIGURES

Figure 2.1: Specimen fabrication WAAM-GMAW process	7
Figure 2.2: Potential domain in WAAM advancement (Chaturvedi et al., 2021).	8
Figure 2.3: Microstructure of WAAM 308 SS characterized at (a) top layer, (b) middle layer, (c) Bottom layer (Li et al., 2021)	10
Figure 2.4: The chemical composition of the employed parent stainless steel wire (Le & Mai, 2020).	11
Figure 2.5: Microstructure of the cross-section stainless steel part and (b) three regions A, B, and C of each deposited layer, Equiaxed grain region (A), Columnar grain region (B), and Fine grain region (C). (Jin et al., 2020)	12
Figure 2.6: Microstructures of WAAM-GMAW thin-walled 308L Stainless Steel in the top zone (Le et al., 2021b).	14
Figure 2.7: Microstructures of WAAM-GMAW thin-walled 308L Stainless Steel in the bottom zone (Le et al., 2021b).	14
Figure 2.8: Microstructures of WAAM-GMAW thin-walled 308L Stainless Steel in the middle zone. (Le et al., 2021b).	15
Figure 2.9: Microstructure of crack boundaries (S. Chen et al., 2022)	16
Figure 2.10: Optically observed porosity for the WAAM 2219 aluminum alloys (Fang et al., 2018).	18
Figure 2.11: Weld beam surface under different welding conditions (Ren et al., 2023)	18
Figure 2.12: Microhardness profile of structure (Vora et al., 2022).	22
Figure 2.13: Humping effect on bead (Lee et al., 2021).	25
Figure 3.1: Flow chart diagram	29
Figure 3.2: 1.2mm 308 stainless steel wire	30
Figure 3.3: GMAW process	33
Figure 3.4: Zeiss EVO Scanning Electron Microscopy (SEM)	35
Figure 3.5: Universal Testing Machine	36

Figure 4.1 Preliminary experiment 1	38
Figure 4.2 Preliminary experiment 2	39
Figure 4.3 Preliminary experiment 3	39
Figure 4.4 Preliminary experiment 4	40
Figure 4.5 Preliminary experiment 5	40
Figure 4.6 Preliminary experiment 6	41
Figure 4.7 Preliminary experiment 7	42
Figure 4.8 Preliminary experiment 8	42
Figure 4.9 Preliminary experiment 9	43
Figure 4.10 Microstructure of 308 SS characterized (a) magnification at 50 $\mu$ m, (b) magnification at 5 $\mu$ m	45
Figure 4.11 Microstructure for deposition layer 308 SS	46
Figure 4.12 Microstructure fracture surface	47
Figure 4.13 Fracture surface at (a) top surface, (b) bottom surface	48
Figure 4.14 Comparison of the mechanical properties tensile test	50
Figure 4.15 Pareto Chart of width effect	51
Figure 4.16 Pareto Chart of height effect	52
Figure 4.17 S/N ratio for width	53
Figure 4.18 Pareto Chart for height	54
Figure 4.19 Regression equation for width	55
Figure 4.20 Regression equation for height	55

## LIST OF ABBREVIATIONS

WAAM	-	Wire Arc Additive Manufacturing
GMAW	-	Gas Metal Arc Welding
SS	-	Stainless Steel
KUKA	-	Keller und Knappich Augsburg
CAD	-	Computer-Aided Design
3D	-	Three-dimensional
ASTM	-	American Society for Testing and Materials
HAZ	-	heat affected zone
UTM	-	Universal Testing Machine
EDM	-	Electrical discharge machining
L	-	Low
UTS	-	Ultimate tensile strength
YS	-	Yield strength
X-ray	-	X-radiation
SEM	-	Scanning Electron Microscopy
DoE	-	Design of Experiment
SE	-	Secondary Electron
BSE	-	Backscattered Electron

## LIST OF SYMBOLS

mm	-	millimetre
g	-	Gram
cm <sup>3</sup>	-	Cubic centimetre
mm/min	-	Millimetre per minute
%	-	Percentage
MPa	-	Mega Pascal
HV	-	Vickers hardness number
wt. %	-	Weight percentage
A	-	Ampere
V	-	Voltage
kV	-	Kilo Voltage
kg	-	Kilogram
μ	-	Micro

# CHAPTER 1

## INTRODUCTION

### 1.1 Background of the study

The study focuses on the microstructure and mechanical properties characterization of Wire arc additive manufacturing with gas metal arc welding for 308 stainless steel in the context of a final-year project. WAAM is a rapidly using arc welding to deposit material layer by layer in an advanced additive manufacturing process, offering the potential for cost-effective production of complex geometries. 308 stainless steel, known for its corrosion resistance and high-temperature properties, is a vital material in various industries, making its optimization in WAAM crucial. Arc additive manufacturing can fabricate or repair fully dense and complex metallic components, reducing manufacturing time and cost. (Chen et al., 2017).

This research aims to experimentally examine how the microstructure and mechanical characteristics of the deposited 308 stainless steel are affected by GMAW-based WAAM process parameters such as welding current, voltage, and welding speed. The study uses a thorough experimental approach to demonstrate connections between process factors and the resultant microstructural properties, such as defect, phase composition, and grain structure. Simultaneously, mechanical testing will reveal information about the material's performance and structural integrity through tensile and hardness tests. The wire feed velocity is the most important of the three input elements for weld bead distance, weld velocity, and voltage flow rate. We may reduce the waviness, porosity, weld fractures, and

weld bead discontinuity of a surface by choosing and optimising the parameters (Vinoth et al., 2022). This study addresses important factors for industrial applications and adds significant information to optimising WAAM procedures for 308 stainless steel.

## 1.2 Problem statement

Wire Arc Additive Manufacturing (WAAM) with Gas Metal Arc Welding (GMAW) for 308 Stainless Steel has gained significant attention in the manufacturing industry due to the potential to revolutionize the production of stainless steel components. Wire arc additive manufacturing is one approach that has the potential to produce substantial metallic structures at cheap costs and high deposition rates. Stainless steels are frequently used due to their superior mechanical qualities and corrosion resistance. Wire arc additive manufacturing (WAAM) is excellent for creating large-scale complicated items because of various benefits, including high disposal rates and cheap costs, so it has become a feasible advanced manufacturing process (Nagasai et al., 2022).

The microstructural characteristics of WAAM-produced 308 stainless steel components, such as grain structure, phase composition, and defects, play a crucial role in determining the material's overall performance and reliability. The mechanical properties, including tensile strength and hardness, are paramount for assessing the structural integrity and functional suitability of the manufactured parts. However, mechanical properties could be improved in the WAAM process. Porosity and cracks are common defects in WAAM processing that need to be minimized because of the adverse effects on mechanical properties, according to (Tomar et al., 2022). Although porosity and cracks have been shown to cause adverse effects, reducing their defect frequency in WAAM remains a persistent challenge. The inherent complexity of the WAAM process, involving intricate interactions between various factors like heat input, travel speed, and material properties, makes controlling defect formation a multifaceted problem. (Jin et al., 2020).

Lack of understanding of the comprehensive relationships between process parameters that can influence the microstructure and mechanical properties of the WAAM process for 308 stainless steel. Studies report the formation of columnar grains with varying ferrite content along the build direction alongside potential defects like porosity and hot cracks. (Kumar et al., 2022). These microstructural features significantly impact the material's strength, ductility, microhardness, and overall performance. These problems include optimizing the parameters of the process by understanding how process parameters such as welding current, voltage, and welding speed can influence the microstructural and mechanical properties of the process.

This study will investigate the problem by understanding the microstructure and mechanical properties of the deposited layer 308 stainless steel. Future research on the characteristics of microstructure and mechanical properties behaviours of WAAM stainless steels is necessary for their potential industrial uses. These components frequently need more adequate or good surfaces, lowering the quality of the metal components. In addition, more work must be done to enhance the WAAM procedure to increase deposition rates and enhance the quality of the WAAM-GMAW fabricated parts of 308 stainless steels.

### **1.3 Objectives**

Objectives of this study are:

- i. To determine the microstructure and mechanical properties of the WAAM-GMAW deposited parts of 308 stainless steels.
- ii. To investigate the effect of process parameters on the bead dimension of the fabricated 308 stainless steel structures.
- iii. To suggest optimized parameters to the bead dimension for 308 stainless steel WAAM process.

## 1.4 Scope of study

The WAAM deposition will be conducted using an EWM GMAW system as a heat source manipulated by a KUKA robot. The material to be deposited is 308 Stainless Steel with 1.2 mm diameter in wire size. The substrate size will be 100 mm in width, 200 mm in length and 10 mm in thickness. The parameters that will be varied are welding current, voltage, and welding speed. The shielding gas will be pure argon. Design of Experiment (DOE), precisely the Taguchi method, will generate the planning matrix unanalysed collected data. The parameter optimization and regression model will be proposed and verified based on the data. The response will be deposition bead height and width. Based on the optimized set parameters, a thin wall will be WAAM deposited at least to a height of 120 mm. Microstructural properties will be analysed using a scanning electron microscope to analyse the microstructure characterization of the deposited 308 stainless steel. Vickers microhardness and Ultimate tensile testing machine will be used to measure the microhardness and tensile properties of the deposited material, respectively.

## 1.5 Significance of study

This study will benefit industries such as additive manufacturing, aerospace, defence, automotive, and manufacturing. The benefits include understanding how deposition parameters affect microstructural and mechanical properties, which can lead to the development of optimized deposition parameters, resulting in improved part quality, performance and reliability. Strength and corrosion resistance are essential qualities that make 308 stainless steel appealing for various applications. This investigation will uncover the complex links between process factors and the final products. This study will pave the way for optimized parameter selection by understanding how process parameters influence bed dimensions. This translates to efficient material deposition, reduced defects, and improved cost-effectiveness of the WAAM process. Additionally, achieving desired bead dimensions directly impacts component geometry and performance, allowing for precise manufacturing and optimized designs.

## 1.6 Research planning

Visual representations of this project's schedule and planning are based on the Gantt chart that coordinates the project's planning activities, and the visual Gantt chart has specific milestones and tasks for each week. Microsoft Excel is the software used to generate the Gantt chart for project planning activities. However, a Gantt chart is required to manage and accomplish the project study within the deadline and timeline. Appendix A shows the Gantt chart of the project activities planning.



## **CHAPTER 2**

### **LITERATURE REVIEW**

#### **1.1 Introduction**

The review explores key studies investigating WAAM processes with various materials, emphasizing those focused on GMAW as the deposition method. Researchers have investigated how welding conditions affect the mechanical characteristics and microstructure of deposited materials, establishing a foundation for understanding the intricacies of the process. Noteworthy contributions discuss the challenges, opportunities, and optimization strategies specific to WAAM-GMAW for stainless steel, setting the stage for the current project. By synthesizing this literature, the study aims to identify gaps, trends, and critical insights that will guide the experimental design and analysis of 308 stainless steel in the context of WAAM-GMAW, contributing to advancing knowledge in this evolving field.

#### **2.1 Wire arc additive manufacturing (WAAM)**

WAAM process has emerged as a significant additive manufacturing process, offering unique scalability, material efficiency, and cost-effectiveness advantages. WAAM involves material deposition between a welding wire and the substrate through an electric arc. This process allows for fabricating large-scale components with intricate geometries, making it particularly relevant in aerospace, automotive, and marine engineering industries.

With minimum energy and material waste, WAAM can build large metallic items faster and cheaply than conventional metal additive manufacturing technologies (Ajay et al., 2023). Because of these innate process advantages, WAAM is a promising manufacturing method for large structural part construction and maintenance in the aerospace, automation, and marine industries. Using an arc as a heat source allows for excellent efficiency in additive manufacturing, making it ideal for producing big and complicated metal objects (Zhang et al., 2024).

WAAM process technology uses an electric arc to melt the metallic wire, which is most used for producing large dimensional parts or components. The choice of the WAAM method directly impacts the deposition rate, time consumed, and processing conditions for a specific material. The WAAM technique has a much higher deposition rate. (Le et al., 2021). A high deposition rate is more suitable for manufacturing metal components produced by the WAAM metal-based process. The WAAM process involves using a welding wire as the feedstock material. The wire is constantly fed into the molten pool formed by the electric arc, solidifying as it melts to achieve the appropriate shape. Wired welding methods are required in the WAAM process for layer-by-layer metal deposition. The manufacturing process is supported by CAD modelling, 3D slicing, and selecting the path to follow. (Kumar et al., 2022). This layer-by-layer deposition enables the fabrication of sophisticated and intricate metal structures that would be difficult or cost-prohibitive to build using existing manufacturing processes. In the WAAM process, metal layers are deposited on top of one another until the required three-dimensional form is produced. Figure 2.1 shows how the wire arc is deposited.

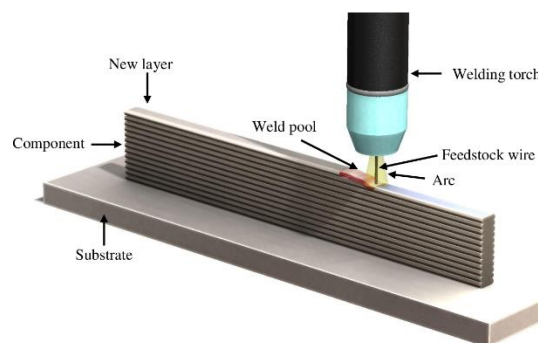


Figure 2.1: Specimen fabrication WAAM-GMAW process

High precision and dimensional accuracy are difficult for WAAM to achieve, and post-processing is frequently necessary for better surface quality. The deposited part may have leftover strains and distortions from the deposition process. Additionally, the technique might not be as suitable for small-scale parts or complicated patterns because of its accuracy limits. WAAM is a promising technique for certain applications, particularly those requiring large and structurally metal components, because of its speed and cost-effectiveness benefits.

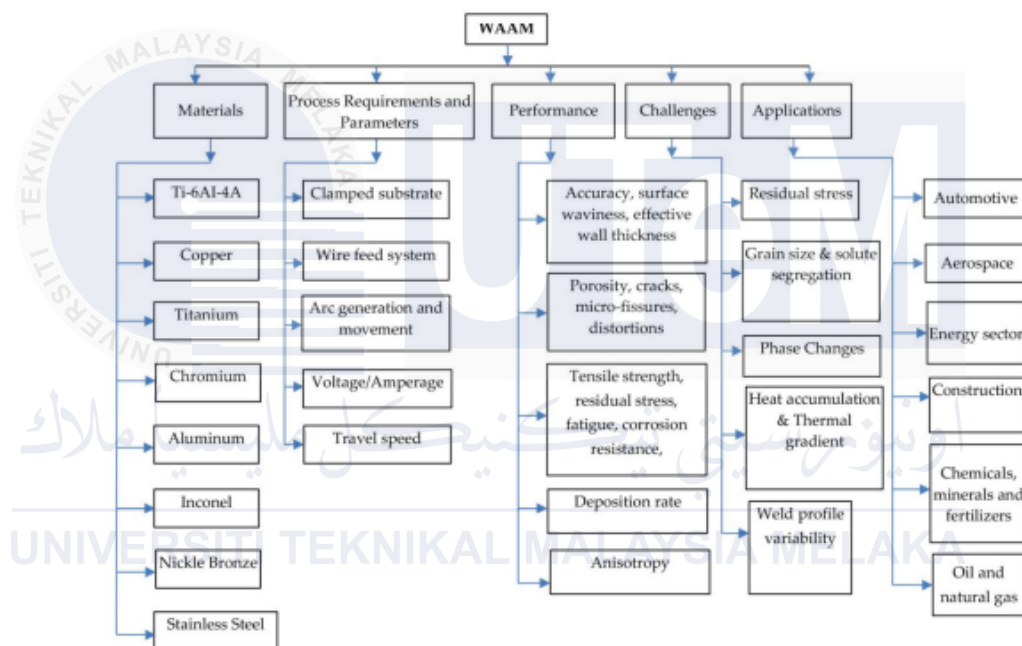


Figure 2.2: Potential domain in WAAM advancement (Chaturvedi et al., 2021).

According to (Chaturvedi et al., 2021) WAAM might investigate novel design strategies to enhance the feasibility of the process for functional material grading and embedded characteristics. To achieve precise control and automation, use controlled mechanisms, parametric optimisation with in-situ monitoring, and non-destructive testing. WAAM is also chosen for its low resource and energy needs. Because of its favourable characteristics, WAAM has potential applications in the aerospace, aviation, automotive, and medical industries. Furthermore, High deposition rates result in lower resolution and a wavy surface finish. Working with WAAM necessitates caution and preparation owing to its high heat input, which restricts material choices.

## 2.2 WAAM applications

This section will cover WAAM for various materials, design arrangements, and application components. WAAM procedures are ideal for materials that have high melting points. This section explains the processes used to produce adequate mechanical characteristics in WAAM-based components. WAAM is a complete system combining task management, wellness tracking, and personalised support features. WAAM caters to your different demands, whether you want to live a better lifestyle, manage your tasks more efficiently, or find a trusted virtual assistant.

(Busachi et al., 2015) They developed a process map for implementing WAAM to produce defence platforms in hazardous situations with mission-critical constraints. The authors reported using a plasma arc with localised shielding, argon recovery equipment, heat treatment, and a fixed gas delivery system. The authors addressed module synchronisation to balance components and jig size and recommended anti-vibration bushes to reduce vibration.

The WAAM approach is ideal for producing large-scale metal objects with near-net form, rapid deposition speeds, and design flexibility (Priarone et al., 2020). Advantages of hybrid manufacturing include reduced fabrication time and waste and the ability to create relatively complicated sections with extended and integrated functions. More research is needed to develop methods for monitoring and controlling in-situ processes while addressing limitations such as residual stress, high heat input rates, and porosity.

## 2.3 Material characteristics

### 2.3.1 308 Stainless Steel

Stainless steel, fabricated by the WAAM technique, has drawn much investigation due to its high ductility and strong corrosion resistance. WAAM can create components with superior mechanical qualities and microstructure that are sound and defects-free. Steel microstructure is predominantly made of austenite phase, however, during WAAM deposition, a mixed microstructure that includes large columnar austenite grains and tiny ferrite grains of skeletal, lathy, and granular forms is created (as shown in Fig. 2.2) (Li et al., 2021).

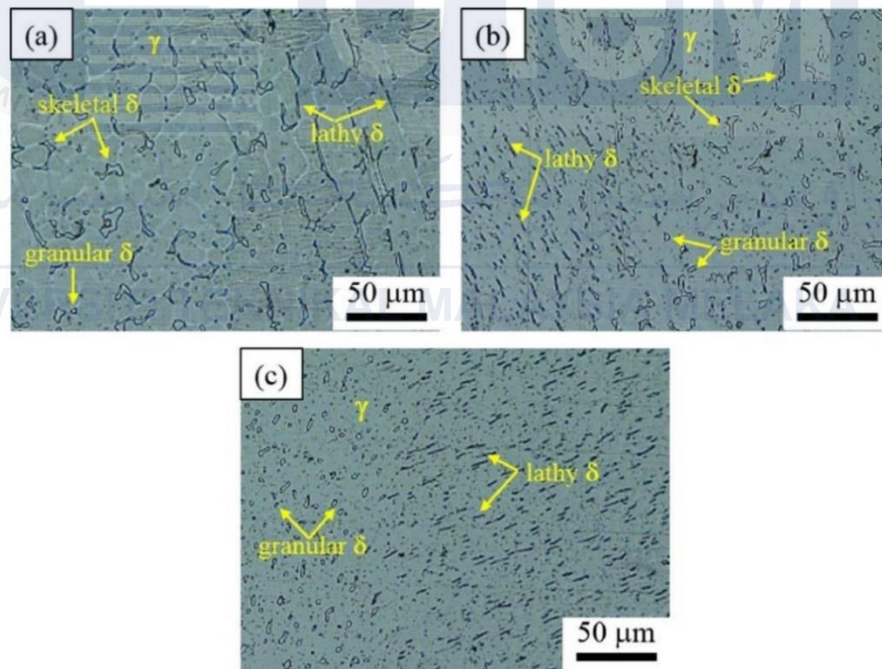


Figure 2.3: Microstructure of WAAM 308 SS characterized at (a) top layer, (b) middle layer, (c) Bottom layer (Li et al., 2021)

Three distinct ferrite grain types are observed: skeletal, lathy, and granular. Additionally, there are apparent differences in ferrite morphology at various levels. For example, the top of the layer is primarily composed of skeletal ferrite, with a small quantity

of granular ferrite structure and lathy ferrite structure. For the steel to behave deformably, the ferrite phase is required, and the thick slip bands that austenite and lathy ferrite produce during deformation are the perfect locations for microcracks to begin. Stainless steel's crystalline structure and alloy composition result in significant deformation behaviour. Its face-centred cubic lattice facilitates twinning and slip processes, which enable plastic deformation. Dislocations inside the crystal lattice migrate in response to mechanical stress, resulting in plastic deformation without appreciable strength loss. Because they include a significant amount of chromium, stainless steel contains high-alloy steels with better corrosion resistance. Their crystalline structure separates them into ferritic, austenitic, and martensitic steels. Stainless steels also include precipitation of hardened steels. These steels have a blend of martensitic and austenitic varieties. Austenitic stainless steels have a wide range of uses. These materials have a wide range of applications because of their superior corrosion resistance, processability, mechanical qualities at low and high temperatures, and durability (Palmeira Belotti et al., 2022). Figure 2.3 shows the chemical composition of 308 L austenitic stainless steel.

Chemical compositions of 308L austenitic stainless steel (in wt. %).

Element	Cr	Ni	Si	Mn	Mo	Cu	C	P	S	Fe
GM-308L wire	19.5–21	9.0–11.0	0.30–0.65	1.0–2.5	0.50 max	0.75 max	0.03 max	0.03 max	0.03 max	Balance
Built 308L wall	19.86	9.84	0.48	1.70	0.0096	0.076	0.021	0.028	0.019	Balance

Figure 2.4: The chemical composition of the employed parent stainless steel wire (Le & Mai, 2020).

## 2.4 Microstructural properties of wire arc additive Manufacturing (WAAM)

WAAM process represents an innovative approach to building three-dimensional metal components layer by layer through the controlled deposition of material using arc welding. The microstructural properties of materials produced through WAAM are pivotal in determining the functional characteristics and mechanical behavior of the final components. The microstructure of WAAM 308 stainless steel walls is mainly composed of residual ferrite that is present in the austenite matrix's grain boundaries and austenite dendrites that develop vertically. Columnar dendrites developing almost vertically comprise

the middle zone, while equiaxed austenite and remnant ferrite phase grains with skeletal and lathy morphologies comprise the top zone (Le et al., 2021).

The top section, middle section, and bottom section parts are the three distinct zones that make up the microstructures. The middle section's mechanical characteristics, microstructure, and macrostructure are essential to the finished parts. The middle zone often experiences the most consistent thermal gradient during deposition, leading to a finer and more equiaxed grain structure compared to the top and bottom (Wang et al., 2016). An increase in strength, ductility, and fatigue resistance is a result of this homogeneous grain structure. Because the substrate cools more quickly and surface contacts have less of an effect, the concentration of defects is smaller than the top and bottom.

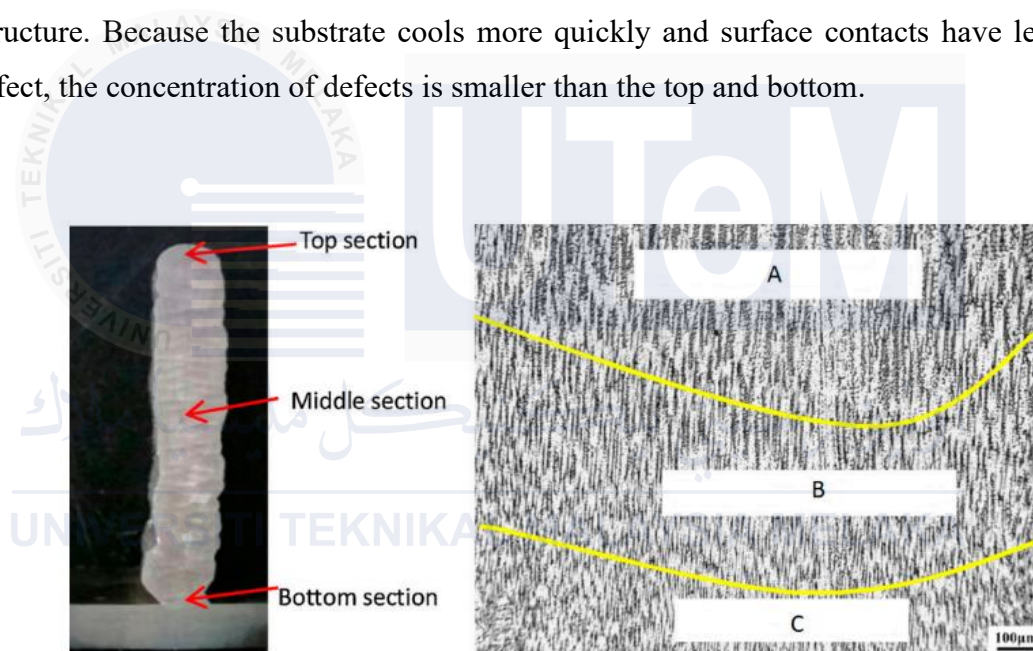


Figure 2.5: Microstructure of the cross-section stainless steel part and (b) three regions A, B, and C of each deposited layer, Equiaxed grain region (A), Columnar grain region (B), and Fine grain region (C). (Jin et al., 2020)

According to (Tomar et al., 2022), Numerous additional factors, including inadequate processing conditions, equipment failures, and ambient factors, are also accountable for other flaws, including oxidation, delamination, and porosity. The mechanical qualities of WAAM-made components are mild compared to their conventionally manufactured counterparts; several flaws are noticed and must be rectified for high-based performance applications. The microstructure of the WAAM process changed dramatically because of the different heat input and cooling rates (Hussein et al., 2021). High heat input is a significant

difficulty in WAAM process-based manufacturing processes because it causes residual stress and deformation in the manufactured structure. One fundamental aspect of the microstructure in WAAM-deposited materials is the grain structure. The rapid solidification process inherent in the welding technique results in a fine-grained microstructure. The size and arrangement of these grains directly impact the material's mechanical properties, including strength and toughness. The WAAM stainless steel products showed significant mechanical anisotropy, with variable characteristics based on test orientation relative to the printing layer direction. Strong crystallographic texture in the microstructure explains the mechanical anisotropy seen (M. T. Chen et al., 2024).

#### 2.4.1 Grain Structure

The microstructure of the WAAM process with GMAW of 308L stainless steel walls varies in size, structure, and morphology from one zone to another zone due to variations in the thermal cycle, temperature gradient, and solidification rate in the top, middle, and bottom zones of the wall. This zone is dominated by columnar dendrites that develop in diverse directions, with a finer grain size than other zones. The rationale follows that that region has the maximum cooling rate because the heat is transported to the cool substrate (Le et al., 2021). Furthermore, when the first layer is deposited and solidifies, the substrate will obtain heterogeneous nucleation and the polycrystalline structure surface, causing dendrites to develop in various orientations and directions. The ferrite phases at the zone are revealed in both the structure of lathy and skeletal morphologies, as shown in Figure 2.5.

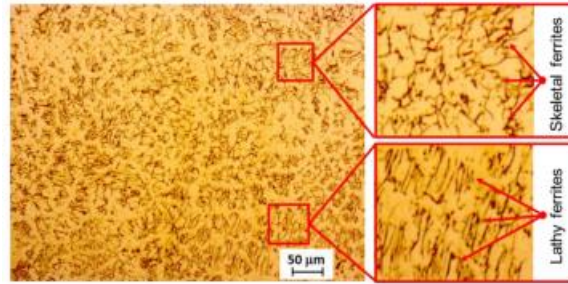


Figure 2.6: Microstructures of WAAM-GMAW thin-walled 308L Stainless Steel in the top zone (Le et al., 2021b).

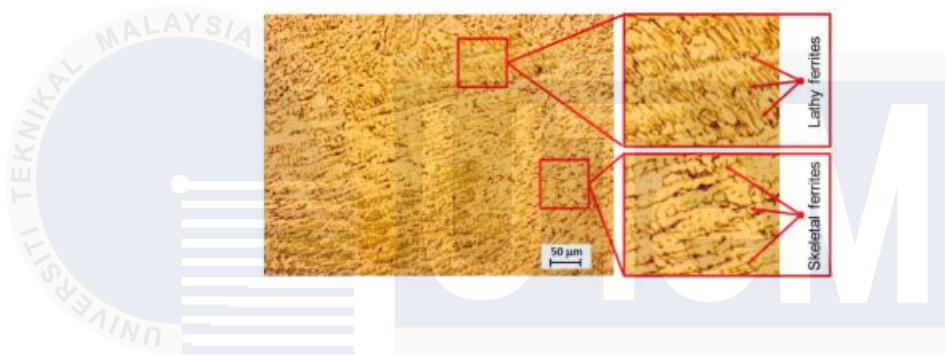


Figure 2.7: Microstructures of WAAM-GMAW thin-walled 308L Stainless Steel in the bottom zone (Le et al., 2021b).

In the case of the top zone, residual ferrite phases with lathy and skeletal morphologies seen at the boundaries of austenite and equiaxed austenite grains make up the microstructure from the middle of the cross-section. In addition, compared to the bottom zone, the grain structure of the zone is coarser. Layer-by-layer preparation causes heat buildup, reducing temperature gradient and solidification rate, leading to coarser columnar dendrites (T. Li et al., 2022). This is because this zone's temperature gradient and cooling rate are smaller than those of the bottom zone. Warmer than the substrate, the layers in the intermediate zone were deposited on top of the previous existing layer. Additionally, heat builds up as the layers that are deposited thicken. Hence, the intermediate zone has a slower cooling rate and a longer solidification period.

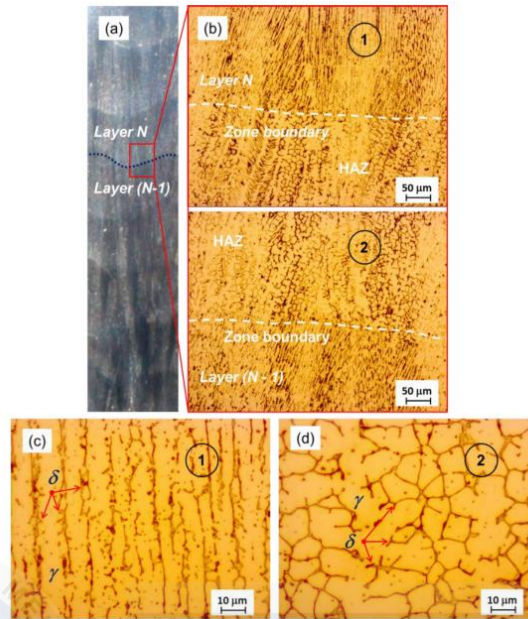


Figure 2.8: Microstructures of WAAM-GMAW thin-walled 308L Stainless Steel in the middle zone. (Le et al., 2021b).

Columnar dendrites, which develop almost vertically, make up the microstructure in the intermediate zone. Furthermore, the heat that creates layer (N) in this zone partially remelts the layer (N-1). Hence, the heat-affected zone (HAZ) between the layers is also observed. The HAZ is often composed of equiaxed grains that are coarser than those found in the body zone (1) of a deposited layer. As a result, a defined layer in the intermediate zone of WAAM-GMAW 308L walls is characterised by finer columnar grains developing almost vertically from the bottom of the layer and then transforming into coarse columnar structures with equiaxed grains at the top (Le et al., 2021). This is because this zone's temperature gradient and cooling rate are smaller than those of the bottom zone. Warmer than the substrate, the deposited layer in the intermediate zone was deposited on top of the previous existing layer. Additionally, heat builds up as the layers that are deposited thicken. Because of this, the intermediate zone has a slower rate of cooling and a longer time for solidification to occur.

## 2.4.2 Crack

A critical factor in the production of cracks is the microstructure of the WAAM-GMAW deposits. Due to its rapid solidification, WAAM-GMAW produces a fine-grained microstructure with a high density of grain boundaries. These grain borders may offer susceptible areas for the development of cracks. Furthermore, some phases in the microstructure can further diminish the fracture toughness and encourage the start of cracks. Cracks are a common type of defect in welds. Various factors, including high heat input, slow cooling rate, and residual stress, can cause them. Cracks can be detrimental to the performance of a weld, and they can also make the weld more susceptible to failure. A crack's microstructure may hold information about its origin. For instance, oxidation during the welding process may be the cause of a fracture that is filled with oxides. A dendritic microstructure-containing fracture might be the outcome of quick solidification. The flaws were found to be intergranular, appearing along high-angle grain boundaries (Seow et al., 2020).

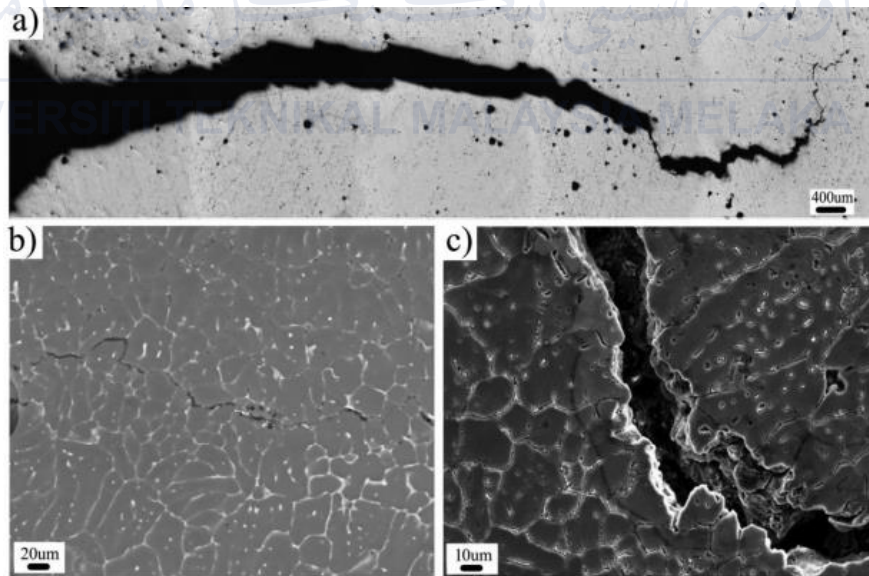


Figure 2.9: Microstructure of crack boundaries (S. Chen et al., 2022)

According to (S. Chen et al., 2022), the WAAM part of alloy with single-pass multilayers. Macro cracks occurred when more than 40 layers were deposited. The thin wall

was fractured in the thickness direction, and the crack spread along the length direction. At increased magnification, the microstructure around the cracks, which included a microcrack and a granular fracture, was visible. The continuous crystalline phase was the light-contrast phase, while the dendrites were the grey-contrast phase. The crystalline phase at the grain boundaries was interrupted, and intergranular cracks, a common characteristic of hot cracks, were seen. The former fracture is primarily dependent on the material's solidification process. It is typically brought on by significant strain in the melt pool or an obstruction in the solidified grain movement (Wu et al., 2018).

### 2.4.3 Porosity

In WAAM fabricated components, A process map can indicate the region where a weld bead deposit is defect-free and steady. Lower heat input techniques may minimise porosity by lowering droplet temperature and gas solubility in the weld pool (Cunningham et al., 2018). Porosity is a defect that can be caused by either raw material or method, and it must be minimised to prevent a negative impact on the mechanical characteristics. It forms because hydrogen gas is trapped in the molten pool during deposition. Such porosity may be controlled using the suitable shielding gas composition and application procedures. Porosity refers to a material's ability to hold air pockets or cavities. Porosity may be a significant problem in wire arc additive manufacturing (WAAM) as it can harm the final components' performance and mechanical characteristics. Gases like oxygen and nitrogen may become trapped in the molten metal during the WAAM process. The metal may subsequently get solidified with these gases, resulting in voids. The metal may contract as it cools and solidifies. If this shrinkage is not adequately accounted for, it may result in voids. One kind of fracture that can happen to metals when heated to high temperatures is called hot cracking. This can occur if the metal cools down too soon or is not heated uniformly in WAAM.

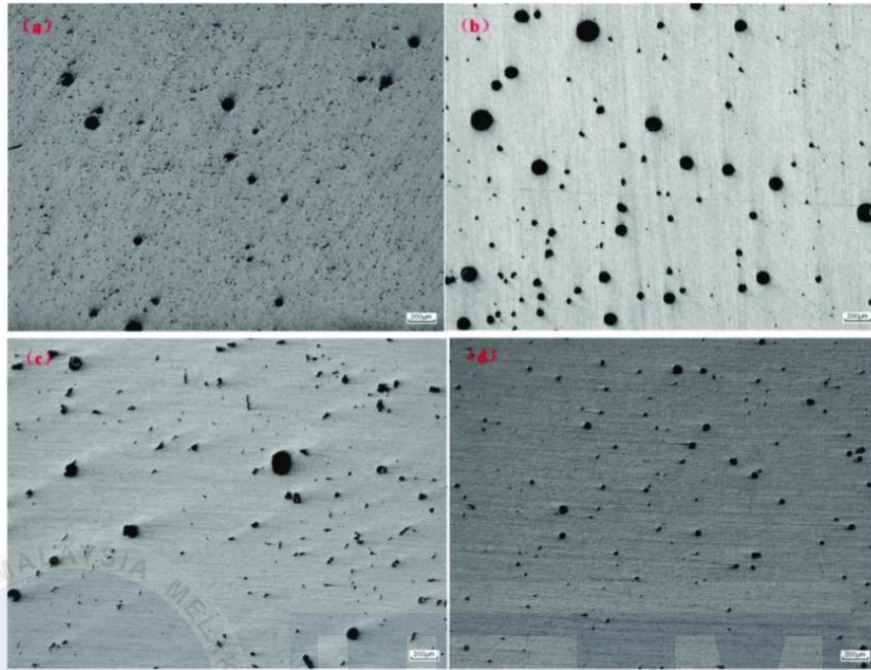


Figure 2.10: Optically observed porosity for the WAAM 2219 aluminum alloys (Fang et al., 2018).

Porosity lowers the components' total density, lowering the produced component's mechanical qualities (such as tensile strength). Due to the different solubility of hydrogen in aluminium in liquid ( $0.69 \text{ cm}^3$ ) and solid ( $0.036 \text{ cm}^3$  per 100 g), hydrogen is one of the primary factors in pore formation during WAAM of aluminium. The wire, which has hydrocarbon impurities, grease, and moisture on its surface, is one of the main sources of hydrogen because it may evaporate in an arc and transform into atomic hydrogen. Process related to the pores are more widely dispersed and may result from the trapping of air (nitrogen and oxygen), shielding gas, or other gases that cannot escape because of the aluminium's quick solidification (Hauser et al., 2021).



Figure 2.11: Weld beam surface under different welding conditions (Ren et al., 2023)

The problem of "stabilising the formation of pores" is said to be resolved by the promoters. Nitrogen pores can be produced with conventional gas metal arc welding. Nonetheless, the discontinuous distribution of tiny holes is visible in the weld seam. According to (Ren et al., 2023), the process of nitrogen pore creation and variables that increase pore appearance were included. Shielding gas was combined with air, nitrogen gas, and water mist during the first phase of the experiment. The air has been selected recently to produce more pores because it has enough nitrogen gas in it to do so economically. The twin-wire arc technique, which has greater spatial adjustability than the single-wire arc process, was employed for further optimise the pores creation based on the influence of the gas pore promoter. The amount of air, the wire feed rate in relation to the arc current, and the welding speed are crucial elements in the development of the pores.

## **2.5 Mechanical properties characterization**

— There is more to characterising the mechanical qualities of WAAM-built buildings than just counting. It explores the complex network of variables that affect and mould these parts' performance. This entails comprehending how the selected metal wire interacts with process variables such as heat input, current, and transit speed to form the underlying microstructure. The ensuing flaws, phase distribution, and grain size have a direct effect on the material's resistance to tensile pressures, which determines whether it is suitable for use in practical applications. Research in this area is actively forging new pathways, continuously refining our understanding of WAAM's mechanical behavior. Studies by (Jin et al., 2020) highlight the mechanical properties characterization of WAAM process of stainless steels can be influenced by various factors, including process parameters, material compositions, and post-heat treatments. Potential of different metal wires, showcasing how understanding their inherent properties can guide us towards maximizing tensile strength within WAAM's capabilities.

## 2.5.1 Tensile Strength

The capacity of a material to withstand deformation under strain before breaking is known as its tensile strength. This corresponds to the highest force a printed part can sustain before coming apart in the context of WAAM. The tensile test is a basic material test used to determine a material's ductility as well as the connection between the material's tensile stress and strain. On a UTM machine, tensile tests were run three times at room temperature for each welding parameter at a ram speed of 2 mm/min. The stress-strain diagram of every sample is provided by the hydraulically powered ram with computerised recording capabilities till it breaks. This type of testing helps determine key characteristics such as ultimate tensile strength, yield strength and elongation, providing insights into the material's performance under tensile (pulling or stretching) forces. Tensile qualities are greater than those of 308 L welding wire and other arc-welding-based additively made 308 L stainless steel products (Nagasai et al., 2022).

Tensile testing was used to evaluate the mechanical characteristics of the multi-layered structure at three separate positions on its top, middle, and bottom sides. In accordance with ASTM E8M, wire cut EDM was used to prepare the specimens for the tensile test. Prior to the fracture, all specimens from the top zone, middle zone, and bottom zones exhibited elastic and plastic deformation. Additionally, a tensile test for wrought SS 316 L was conducted. The findings show that the wrought SS 316 L has a percentage elongation of 45%, an ultimate tensile strength of 485 MPa, and a yield strength of 220 MPa. Three sample tensile test specimens taken from the multi-layered construction were used to compare these values of tensile characteristics with the outcomes.

Table 2.1: Tensile properties of GMAW-AM 316 L and wrought 316 L. (Vora et al., 2022)

Property	UTS (MPa)			YS (MPa)			Elongation (%)		
	Top	Middle	Bottom	Top	Middle	Bottom	Top	Middle	Bottom
Sample									
Experimental value	520.6	512.7	504.29	268.6	249.26	251.85	48.98	49.72	49.36
Average value	512.53			256.57			49.35		
Wrought 316L values	485			220			45		

The tensile test findings for the three multi-layered construction specimens and the wrought 316 L are summarised in Table 2.1. For the ultimate tensile strength, yield strength, and elongation, the average of the top zone, middle zone, and bottom zone value specimens was 512.53 MPa, 256.57 MPa, and 49.35%, respectively. The wrought SS 316 L range values correspond to the experimentally observed UTS, YS, and Elongation of the components produced by the WAAM process. Compared to wrought 316 L, each top, middle, and bottom zone has unique values and has demonstrated strong tensile capabilities. The GMAW-based WAAM method component meets the specifications for commercial usage since all tensile parameters support the industrial necessity for SS 316 L (Vora et al., 2022).

While WAAM offers significant advantages for large-scale metal manufacturing, further study and development are required to realise its full potential in terms of generating tensile strength that is dependable and constant. WAAM may be further optimised for more demanding applications by investigating novel ways and comprehending the critical aspects controlling this important attribute.

### 2.5.2 Microhardness

WAAM-GMAW deposits a continuous wire electrode layer by layer, providing perfect control over the deposition process. Welding settings, heat input, and cooling rates all influence the microhardness of the final structure. The localised heat created during welding causes quick solidification, influencing the microstructure and, ultimately, the microhardness distribution. Higher ferrite concentration and smaller grain size may contribute to increased hardness in the WAAM process (Huang et al., 2023). Stainless steel, recognised for its corrosion resistance and mechanical strength, has changing microhardness values throughout its construction due to solidification and cooling dynamics. Fine-tuning welding parameters such as voltage, current, and travel speed allows for the optimisation of microhardness profiles throughout the construction. Achieving a balanced microhardness distribution is critical for ensuring uniform strength and endurance of the manufactured components. According to (Vora et al., 2022), the figure shows the correlation between

microhardness and measurement with different locations for multi-layered structures in the top zone, middle zone, and bottom zone. The average microhardness values in the top, middle, and bottom zones were 177.45 HV, 180.82 HV, and 184.25 HV, respectively. The bottom zone has stronger microhardness than the top and middle zones, although only slightly. The bottom zone of the construction, which represents the initial layer, was applied to the base plate and heat-affected zone. Microhardness values were constant across the structure, including all zones. The uniform microhardness grade suggests that it will not result in brittle failure.

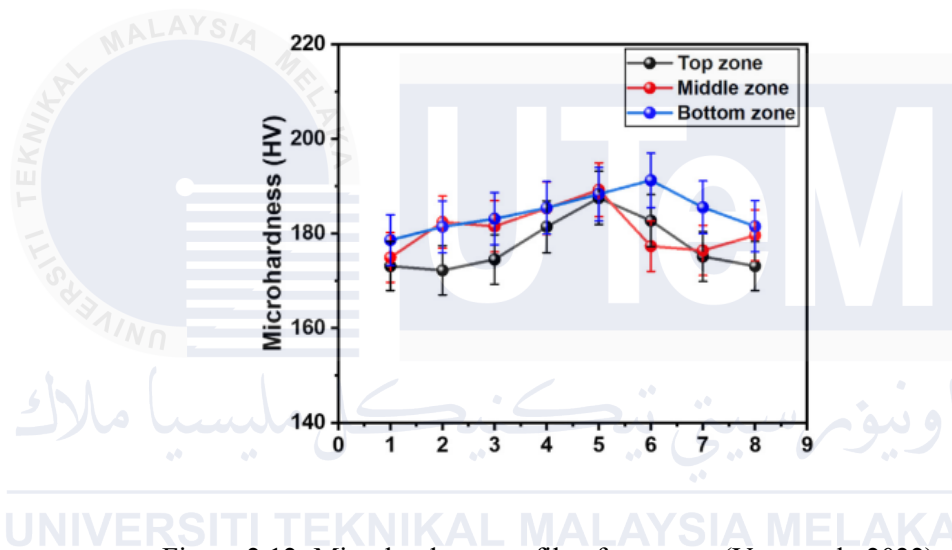


Figure 2.12: Microhardness profile of structure (Vora et al., 2022).

## 2.6 Process parameters of wire arc additive manufacturing

The process parameters employed in WAAM are critical factors influencing the quality, efficiency, and characteristics of the manufactured components. These parameters include the wire feed rate, travel speed of deposition, and voltage/current settings regulating the heat input and arc stability. Travel speed impacts cooling rates and microstructure, while layer height or bead width contributes to the overall resolution and surface finish of the printed part. These factors will directly impact weld properties and the quality of the deposited structure since they all affect the heat input of the deposition (Tomar et al., 2022).

### 2.6.1 Heat input

Heat input in the WAAM significantly impacts the melt pool size. The width-to-height ratio is substantially less at lower heat inputs because the melt pool does not have sufficient time to expand before solidification (Tomar et al., 2022). Increasing heat input makes the metal less viscous, and the melt pool expands more readily. However, by matching the cooling power with the heat input, the heat dissipation disparity between two subsequent layers may be reduced, and constant bead form may be produced. Programmes for synergistic welding offer reliable welding procedures for a particular material in single-pass welding or for substrates at room temperature. High heat input can produce a broader and deeper bead because it can promote more fusion and penetration. On the other hand, problems, including deformation, residual strains, and even metallurgical changes, might also result from overheating. Low heat input, on the other hand, may result in insufficient layer bonding and fusion. Equation 2.1 shows the heat input per unit deposition (Shukla et al., 2023).

$$\text{Heat Input} = \frac{\text{Power}}{\text{Welding Speed}} \quad \text{Equation 2.1}$$

Achieving the appropriate microstructure and mechanical qualities in the finished item requires precise control over the amount of heat input. It is essential in avoiding problems like porosity, deformation, and cracking (Wang et al., 2016). Optimising heat input makes finding the ideal balance between deposition efficiency and preserving the deposited material and structural integrity more accessible. It is essential to consistently monitor and modify welding conditions to regulate heat input and guarantee the creation of high-grade and precisely dimensional components.

### 2.6.2 Welding speed

Welding speed refers to the rate at which the welding torch traverses the workpiece during additive manufacturing. This parameter directly affects the build-up geometry, thermal interactions, and material deposition, among other important elements of WAAM. Selecting the ideal welding speed requires careful consideration of several variables, including heat input, cooling rates, and the solidification behaviour of the deposited material. Additionally, (Zhou et al., 2020) highlighted the influence of electric arc travel speed on the microstructure and mechanical properties of additively manufactured parts. Collectively, these studies underscore the importance of welding speed in wire arc additive manufacturing. As a result, using WAAM's full potential necessitates a careful consideration of welding speed. While faster speeds indicate more efficiency, going above key thresholds might endanger the build's structural integrity. The key to achieving the ideal balance between speed and quality is carefully adjusting process parameters to suit the material and intended use.

### 2.7 Effect of process parameters on bead quality

When combined with gas metal arc welding (GMAW), the wire arc additive manufacturing (WAAM) technique offers significant advantages in terms of cost-effectiveness and design freedom. The growing need for sophisticated production methods makes comprehending the complex interactions between process variables and bead quality critical. Several process factors are closely related to the quality of deposited beads in WAAM with GMAW. Elements, including wire feed rate, welding current, arc voltage, travel speed, and layer height, are important factors that affect the mechanical characteristics, microstructure, and geometry of the bead deposits. According to (Ana Rosli et al., 2020), As the printing speed increases, the breadth of the deposited layer decreases. This is because increased travel speeds increase the cooling rate while decreasing the ratio of temperature gradient to solidifying development. The decrease in heat buildup with increased speed causes the breadth of the deposits to shrink, as seen by the evolution of geometric properties. As the heat input decreases, an uneven bead deposit also forms, creating a flaw between the

layers known as humping. One of the frequent flaws in welding is humping, which stops additional deposition operations.

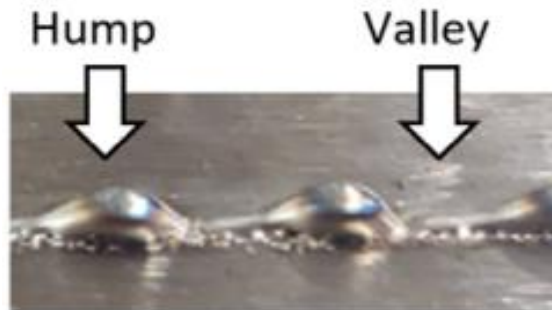


Figure 2.13: Humping effect on bead (Lee et al., 2021).

Wire feed speed directly impacts the amount of material deposited in a unit of time. The overall structural integrity of the deposited layers may be impacted by uneven bead production caused by wire feed speeds that are too high or too low. The amount of energy used in the welding process is affected by arc voltage. Changes in the arc voltage can affect the penetration, fusion, and breadth of the bead on the substrate. Uneven deposits were also discovered at lower welding power and higher wire feed rates due to an abundance of material in the melt pool at lower power (S. Chen et al., 2022).

These process parameters must be optimised to obtain consistent bead morphology, appropriate fusion, and acceptable mechanical characteristics. As part of WAAM-GMAW, these parameters are continuously monitored and adjusted to maintain constant bead quality and to help produce high-quality, dependable, additively produced components.

## 2.8 Defect analysis

The process may reveal several defects. Microstructural issues include variations in grain size, dendritic solidification, and potential porosity due to rapid solidification during

layer deposition. Mechanical property challenges involve anisotropic behavior, residual stresses, and inconsistent hardness across layers. Inclusions or lack of fusion can compromise mechanical integrity. Thorough defect analysis using metallography, X-ray imaging, and mechanical testing is essential. Optimizing process parameters, heat treatment, and post-processing steps becomes crucial for mitigating defects and achieving the desired microstructural and mechanical properties in WAAM-GMAW-fabricated 308 stainless steel components.

For high-performance applications, solving the numerous defects identified in WAAM-made components is necessary, even though their mechanical qualities are somewhat modest compared to their conventionally manufactured counterparts. Because it causes a high degree of distortion and residual stress in the manufactured structure, excessive heat input poses a significant barrier to WAAM-based fabrication procedures. A major worry for dimensional compatibility and early component failure is the lower surface quality of the WAAM-fabricated components because of the high heat input. Porosity, delamination, and oxidation can also be caused by various other factors, including improper processing settings, machine faults, and environmental influences (Tomar et al., 2022).

## CHAPTER 3

# METHODOLOGY

### 3.1 Introduction

The methodology and process utilised for the research in this experiment. The design of the experiment, the workflow, the setup of the experiment, and the data analysis that will be utilised are all specifics of the experimental methodology that will be utilised in this study. Furthermore, the analysis and methodologies used were selected considering previous research. Through experiment setup and analysis, this research will also contain an introduction to the techniques and methods for the mechanical properties and microstructure of deposited 308 stainless steel. A well-thought-out plan for the project's flow was implemented with pertinent flow charts, experiment designs, and processes that standardise research reporting.

### 3.2 Gantt chart

Table 3.1: Gantt Chart PSM 1

TASK	WEEK														
	1	2	3	4	5	6	7	8	9	10	11	12	13	14	15
PSM 1 Title Selection	█														
PSM 1 Title Conformation		█													
Discussion about the project with Supervisor			█												
Search for Relevant information of Journal and Articles			█	█											
Chapter 1 (Introduction)				█	█										
Chapter 2 (Literature Review)				█	█	█									
Chapter 3 (Methodology)							█	█	█						
References And Formatting											█				
Submission of Log Book to Supervisor												█			
Submission of General Conduct Form													█		
Poster Presentation														█	
Complete PSM 1 Report															█
Final Report Submission															█

Table 3.2: Gantt Chart PSM 2

TASK	WEEK														
	1	2	3	4	5	6	7	8	9	10	11	12	13	14	15
PSM 2 Briefing	█														
References And Formatting		█													
Briefing by Laman Hikmah			█												
Lab progress			█	█	█	█	█	█	█	█	█	█	█	█	
Chapter 4 (Result and Discussion)						█	█								
English technical talk									█						
Technical report										█					
Submission of Log Book to Supervisor											█				
Project oral Presentation PSM 2												█			
Preparing Project report													█	█	█
Project report submission to examiner															█
Final report PSM 2 submission to supervisor															█
CD submission of PSM 2 to faculty															█

### 3.3 Flow chart

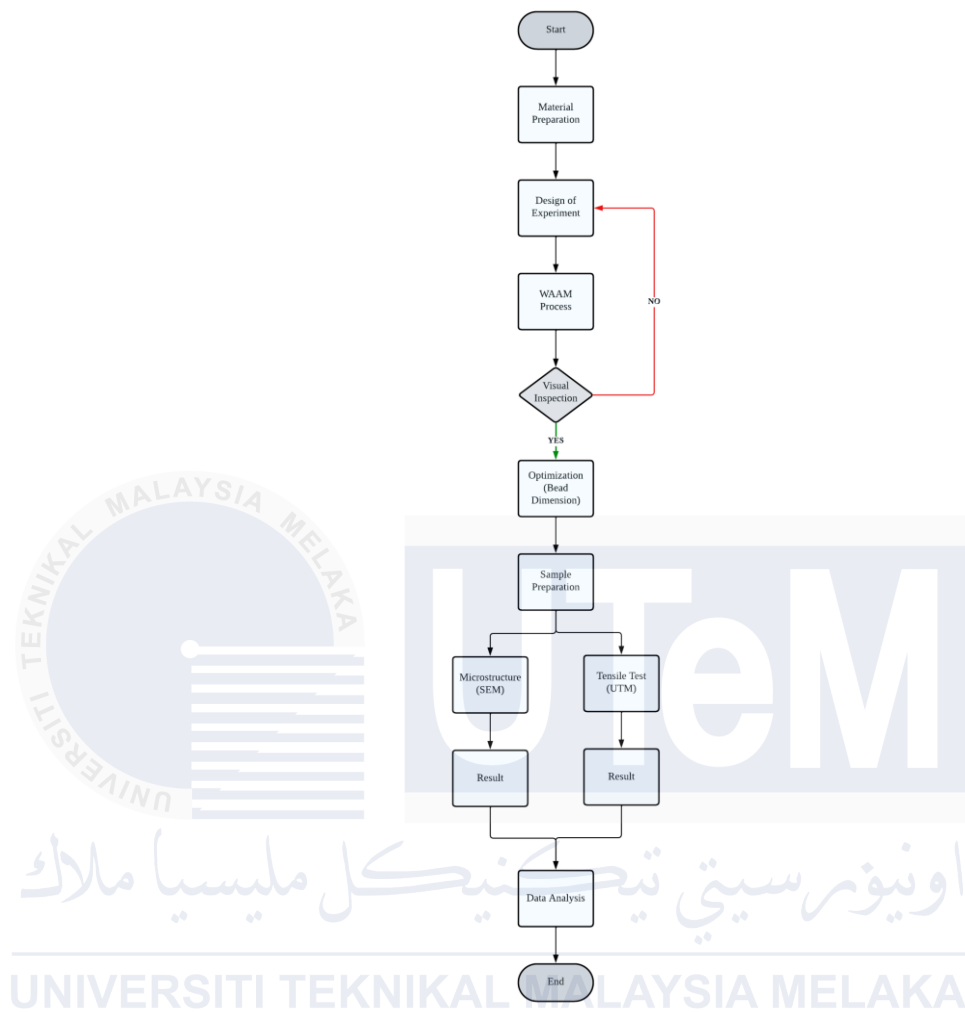


Figure 3.1: Flow chart diagram

### 3.4 Material Preparation

#### 3.4.1 308 stainless steel wire

The wire shows in figure material selected for the experiment was 308 stainless steel. The wire was a 1.2 mm diameter solid wire of 308 Stainless Steel. The chemical composition of this wire is shown in the table.



Figure 3.2: 1.2mm 308 stainless steel wire

Table 3.3: Chemical composition of 308 Stainless steel

Carbon	0.8 max
Chromium	19.0 – 21.0
Nickel	10.0 – 12.0
Manganese	2.0 max
Silicon	0.75 max
Phosphorus	0.045 max

### 3.5 Design of Experiment (DoE)

The parameters such as welding current, voltage and welding speed, as shown in the table, are the factors influenced by the microstructure and mechanical properties of the WAAM process with GMAW for 308 stainless steel that will be investigated in this project. There are 3 variables, as shown in the table below. This parameter and variable for the optimization of process parameters in the experiment deposited layer of 308 stainless steel will be used in the design of the Experiment (DoE).

Table 3.4: Variable for process parameters

Welding Parameters	Low	Medium	High
Welding Current, I (A)	120	130	140
Voltage, V (V)	18.0	18.5	19
Welding Speed, v (m/min)	0.2	0.3	0.4

### 3.5.1 Taguchi Method

The Taguchi method offers a powerful approach to optimize the WAAM process with GMAW for 308 stainless steel, focusing on both microstructure and mechanical properties. Taguchi, a robust optimization method, helps identify key GMAW parameters influencing microstructure and mechanical properties of WAAM deposited 308 stainless steel. Strategically assigning 3 Parameters (welding current, voltage, welding speed) into an L9 orthogonal array efficiently assigns factor combinations to minimize experimental runs while maintaining statistical significance. The experiment design using the L9 Orthogonal Array is shown in Table.

Table 3.5: Design of Experiment

Experiment	Welding Current (A)	Voltage (V)	Welding Speed (m/min)	Width (cm)	Height (mm)
1	120	18	0.2		
2	120	18.5	0.3		
3	120	19	0.4		
4	130	18	0.3		
5	130	18.5	0.4		
6	130	19	0.2		
7	140	18	0.4		
8	140	18.5	0.2		
9	140	19	0.3		

### 3.6 WAAM Process

Wire Arc Additive Manufacturing (WAAM) for 308 stainless steel, Gas Metal Arc Welding (GMAW) employs layer-by-layer material deposition to produce three-dimensional structures. In this process, a KUKA robot is equipped with a welding torch, and a continuous wire electrode is fed through the torch. The robot precisely manipulates the welding torch, following a programmed path to deposit molten metal onto the workpiece. The GMAW process uses an inert argon gas to protect the weld pool from airborne impurities and provide a clean, high-quality weld. The electrical energy required to melt the electrode and form the weld bead is supplied by a power source.

This experiment used GMAW to deposit the WAAM technique on 308 stainless steel. Procedure where the workpiece metal and a consumable wire electrode create an electric arc that heats the metal and causes it to fuse or melt and combine. The shielding gas that passes through the welding torch and the wire electrode protects the process from air contamination. Although alternating current and constant current systems can also be used, constant voltage

and direct current are the most used power sources for GMAW. The four primary methods GMAW uses for metal transfer are pulsed spray, short-circuiting, globular, and spray. Every technique has distinct qualities, advantages, and disadvantages.

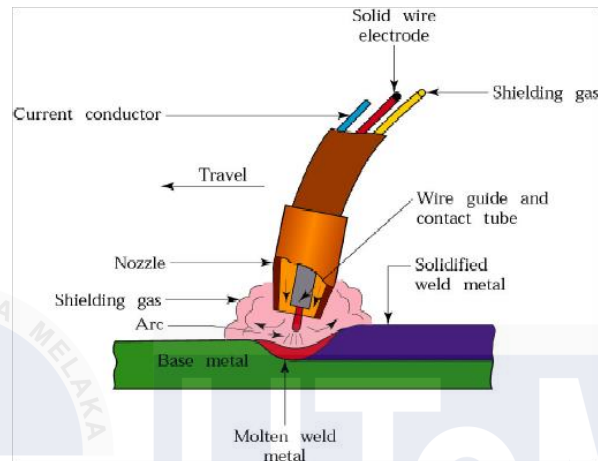


Figure 3.3: GMAW process

### 3.7 Experiment Method

In this experiment, 308 Stainless Steel with diameter of 1.2 mm and using 304 stainless steel base plate (150 mm X 25 mm X 12 mm) in length, width and thickness were used in the GMAW robot according to WAAM process. During welding process, the argon gas applied into the shielding gas and after finished the deposition, the specimen was cooled down in room temperature. The process parameters optimization for the deposited layer from the previous study method above has been used in this experiment. Minitab software generated the selected parameters and variables from the optimization of welding current, voltage and welding speed based on the Taguchi method. Wire cut EDM used to cut the specimen sample for microstructure and mechanical testing. ASTM E8/8M specimen sample was used in this experiment. Scanning electron microscopy (SEM) for microstructure analysis and 100KN UTM tensile testing for mechanical testing.

### 3.7.1 Analysis of the deposition geometry

In the WAAM process, 308 stainless steel wire was deposited onto a 304 stainless steel base plate. This research investigates the effect of parameters on deposition geometry and is executed according to the design matrix generated through Minitab software. The preliminary experiment used 3 layers of deposition to gather layer-by-layer effects through which width and height could be observed. The responses, which were width and height, were measured then using vernier callipers and welding gauge as shown in figure 3.4.

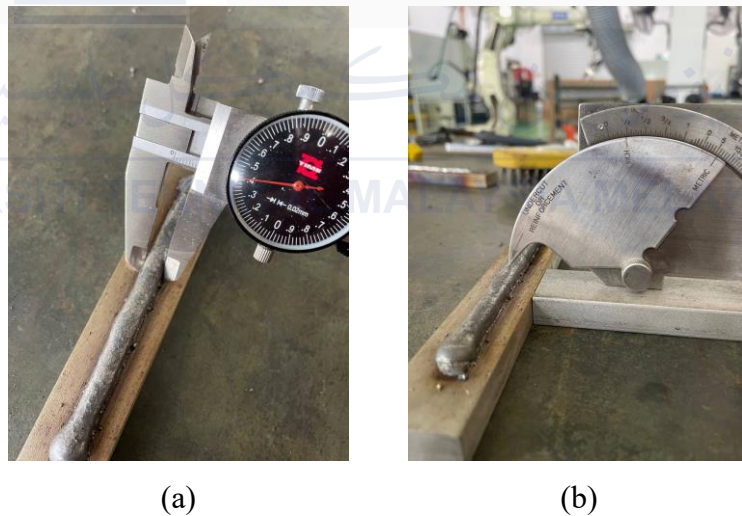


Figure 3.4: (a) vernier calliper and (b) welding gauge

### 3.7.2 Microstructure (SEM)

The experiment used Scanning Electron Microscopy (SEM) to analyse the microstructure of the layer of 308 stainless steel that had been deposited. Describing the microstructure of the layer deposited in 308 stainless steel produced using GMAW in Wire Arc Additive Manufacturing (WAAM) is essential.



Figure 3.5: Zeiss EVO Scanning Electron Microscopy (SEM)

In the SEM chamber, place the mounted and etched sample. Depending on the required resolution and magnification, choose the correct working distance (10–20 mm) and accelerating voltage (15–20 kV). Secondary Electron (SE) imaging. The topography of the sample may be seen in high-resolution photographs using this standard mode, which also makes surface characteristics like grain size, morphology, fractures, porosity, and precipitates visible. Backscattered Electron (BSE) imaging. This mode emphasises variations in atomic weight according to picture brightness. It facilitates the identification of inclusions or precipitates as well as phase distinctions. For example, austenite appears brighter than ferrite.

### 3.7.3 Tensile Testing

Tensile testing is key to assessing the mechanical characteristics of WAAM-produced 308 stainless steel within the larger characterization process. This experiment was carried out to analyse the ultimate tensile strength, yield strength, and elongation at fracture.



Figure 3.6: Universal Testing Machine

Select appropriate load to pull the specimen till it breaks using the UTM. Make that the device is correctly calibrated and operating. Choose grips that are suitable for the specimen's shape and composition. For metals, flat grips with serrations are frequently utilised. More precise strain data can be obtained by using an extensometer to measure the specimen's elongation directly during the test.

Carefully mount the specimen in the grips of the UTM, ensuring proper alignment and centring. Without crushing the specimen, firmly tighten the grips. To eliminate any slack in the testing apparatus and guarantee correct contact between the specimen and grips, provide a tiny pre-load. Adjust the test settings based on the selected standard or your requirements. Usually, this entails figuring out the strain rate. As soon as the test is underway, begin recording the force and displacement data. Test the specimen continuously until it cracks. Measure the final gauge length and note the fracture appearance after the test.

## **CHAPTER 4**

### **RESULT AND DISCUSSION**

#### **4.1 Introduction**

This chapter presents the findings of the experimental design. This chapter also includes the study's findings and discoveries. This chapter also includes data analysis for the experimental design. The major focus of this work is on the microstructure and mechanical characteristics of 308 stainless steel. The process factors that impact bead diameters and shape have also been explored. This process's parameters include welding current, voltage, and speed. This parameter is not independent. The parameters have also been optimised to indicate the deposition of 308 stainless steel utilising wire arc additive manufacturing using the GMAW process.

#### **4.2 Preliminary Experiment**

Table 4.1 shows of welding parameters for Wire Arc Additive Manufacturing (WAAM) of 308 stainless steel. The Design of Experiment (DOE) of this study were conduct by using Taguchi method. This method was used to perform a optimal setting of parameter deposition of 308 stainless steel. 3 layers of deposition will be run for each sample run.

Table 4.1: Design of Experiment using Taguchi method

Experiment	Welding Current (A)	Voltage (V)	Welding Speed (m/min)
1	120	18	0.2
2	120	18.5	0.3
3	120	19	0.4
4	130	18	0.3
5	130	18.5	0.4
6	130	19	0.2
7	140	18	0.4
8	140	18.5	0.2
9	140	19	0.3

This section describes runs using the design of experiment (DOE) parameters above. In this section, the dimension of bead geometry one of the components that will be focused on in this preliminary experiment.



Figure 4.1: Preliminary experiment 1

Figure 4.1 illustrates the first sample of preliminary experiment. For this experiment, the deposition figure 4.1 used the lowest welding level of parameter, 120 A current, 18 V

voltage and 0.2 m/min for welding speed. From the result, the deposition was not stable and have welding spatter imperfection because of welding voltage was too low.



Figure 4.2: Preliminary experiment 2

Figure 4.2 shows the second sample of preliminary experiment. For this experiment, the parameter deposition was change to 120 A current, 18.5 V voltage and 0.3 mm/min for welding speed. From the result, the deposition was proved that increasing the welding current and voltage make the deposition bead smoother and reduce the welding spatter imperfection the width of the bead dimension reduces because of the welding speed increased.



Figure 4.3: Preliminary experiment 3

Next, for third sample shown in figure 4.3, the parameter was change to 120 A current, 19 V voltage and 0.4 m/min. From the result, the deposition bead dimension reduce because of the welding speed was increase. This proved that increasing the welding speed make the deposition bead the width and height t of the bead dimension reduces.



Figure 4.4: Preliminary experiment 4

Figure 4.4 shows the result that be set of parameters which was 130 A current, 18 V voltage and 0.3 m/min of welding speed. This sample of preliminary experiments gave a unstable welding bead where the starting of deposition gave a better welding bead while at the end of the deposition was unstable. This is because of the increased of welding current that make the voltage and welding speed was not consistent.



Figure 4.5: Preliminary experiment 5

Change was made in following sample shown in figure 4.5 by increasing the 18.5 V voltage and 0.4 m/min welding speed. The welding current remain same as previous experiment. The change of parameters resulting the decrease in width of bead dimensions. This proved that welding speed affect the width of bead dimensions. The deposition was smoother than previous sample due to changes in voltage of parameter.



Figure 4.6: Preliminary experiment 6

For next sample that shown in figure 4.6, increasing the 19 V voltage resulting the bead dimension wider than the previous sample. The quality of the bead dimension not consistent and thicker because of the welding speed was change to 0.2 m/min welding speed. This result showing reduce the quality of deposition.



Figure 4.7: Preliminary experiment 7

Figure 4.7 changed to 140 A current, 18 V voltage and 0.4 m/min for welding speed. From the result, the dimensions width of bead thinner because of welding speed. The welding deposition has smoother due to high current of deposition parameters but the welding was not consistent.



Figure 4.8: Preliminary experiment 8

The result in figure 4.8, the welding voltage and speed was changed to 18.5 V and 0.2 m/min while the welding current same as previous sample. This sample experiment resulting the width of the bead increase because of the welding speed and the deposition bead was not consistent as previous sample.



Figure 4.9: Preliminary experiment 9

During last run of preliminary experiment shown in figure 4.9, the welding current same parameter as previous and the changed of 19 V voltage and 0.3 m/min, which give the best quality of deposition. It showed the better welding result when changing the voltage and welding speed of parameters. The deposition was more consistent and smoother than previous sample of preliminary experiments. This sample resulting the best parameters for 308 stainless steel deposition.

### 4.3 Design Matrix

The table 4.2 displays the design matrix created by the Minitab Software. In this research, the experiment for the parameters factor was constructed using L9 orthogonal array configurations for 9 sample runs. The experiment was carried out by executing the design matrix created by depositing 308 stainless steel utilising the GMAW method. This experiment consisted of three layers of deposition, each having a step height of 2 mm. It was intended to investigate the layer-by-layer deposition of 308 stainless steel wire. As a result, the width and height dimensions of the beads were measured in response to this data. The table 4.2 shows the measurement results that were recorded.

Table 4.2: Design matrix

Experiment	Welding Current (A)	Voltage (V)	Welding Speed (mm/min)	Width (cm)	Height (mm)
1	120	18	0.2	0.945	7
2	120	18.5	0.3	0.84	6
3	120	19	0.4	0.756	5.5
4	130	18	0.3	0.908	6
5	130	18.5	0.4	0.752	6
6	130	19	0.2	1.202	7
7	140	18	0.4	0.814	7
8	140	18.5	0.2	1.218	7
9	140	19	0.3	0.98	6.5

#### 4.4 Relationship parameters and response

The deposition properties of 308 stainless steel in Wire Arc Additive Manufacturing (WAAM) employing Gas Metal Arc Welding (GMAW) are considerably influenced by a variety of factors. The table 4.2 illustrates that raising the welding current and voltage results in a wider and higher deposition. For example, experiments 6 and 8 with 130 A and 140 A currents, respectively, had widths of 1.202 mm and 1.218 mm, and heights of 7 mm apiece. In contrast, greater welding rates tend to reduce the deposition width and height, as illustrated in experiment 5 with a speed of 0.4 mm/min, producing a width of 0.752 mm and a height of 6 mm. Optimal parameter selection is critical for obtaining the required deposition geometry for large metallic structures in manufacturing industries application.

## 4.5 Microstructural analysis

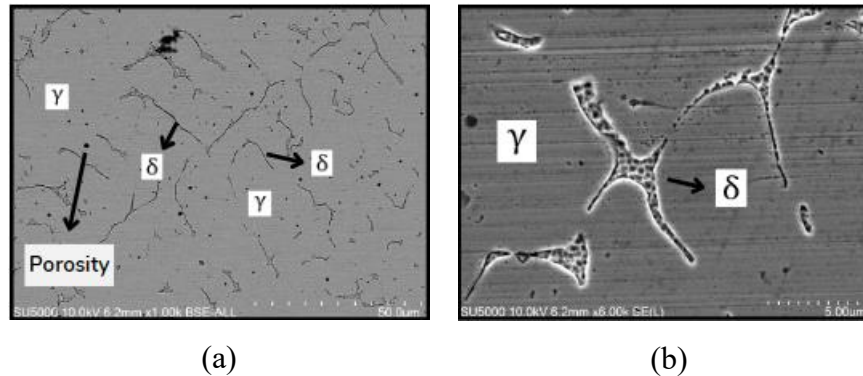


Figure 4.10: Microstructure of 308 SS characterized (a) magnification at 50µm, (b) magnification at 5µm

The first figure 4.10 (a), taken at higher magnification at 50µm reveals a heterogeneous microstructure comprised of austenite ( $\gamma$ ) and ferrite ( $\delta$ ). This dual-phase structure is typical of 308 stainless steel and adds to its mechanical qualities. The austenitic phase ( $\gamma$ ) is ductile and tough, whereas the ferritic phase ( $\delta$ ) is strong and resistant to cracking. The existence of porosity, as seen in the figure, is a typical problem in WAAM techniques and can have a substantial impact on mechanical characteristics. Porosity is mainly caused by gas entrapment during the rapid solidification process. It displays a two-phase structure of austenite and ferrite with varied porosity. With a fine-grained structure with well-distributed ferrite increasing strength and a balanced austenite-ferrite ratio improving ductility. When the cooling rate surpasses a certain limit, the  $\gamma$  morphology, which may be called the primary phase, outperforms the ferrite morphology due to variations in dendrite cooling by (Le & Mai, 2020). The second figure 4.10 (b) shows a closer look at 5µm for the microstructure, highlighting the intergranular dispersion of ferrite within the austenitic matrix. The ferritic areas show as elongated or lath-like structures inside the austenitic grains, which add to the material's overall strength. This distribution reflects a solidification process that resulted in the production of ferrite along grain boundaries, which can assist reduce grain boundary movement and improve the material's high-temperature properties.

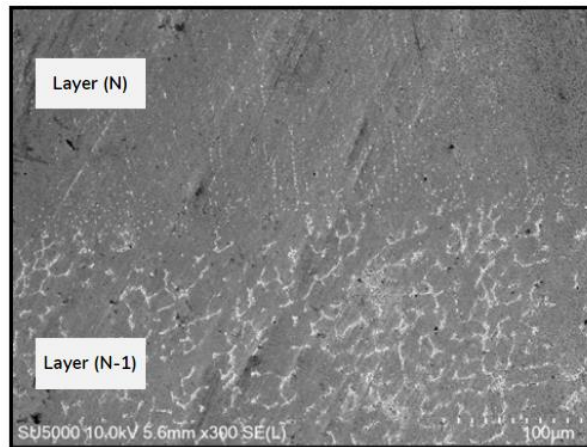


Figure 4.11: Microstructure for deposition layer 308 SS

The figure 4.11 shows a view of the microstructure at lower magnification, demonstrating the material's general uniformity. The grain boundaries are more evident here, indicating a finer-grained structure. Fine grains are frequently associated with enhanced strength and toughness because they provide more grain border area, slowing dislocation movement. Furthermore, the previously deposited layer (N-1) is partially remelted by temperature, making the ferrite phase coarser. Slower cooling might result in coarser structures and more delta ferrite. The deposited layer (N) has finer ferrite due to quick cooling, mostly consists of columnar dendrites that develop along the building direction.

## 4.6 Fracture surface analysis

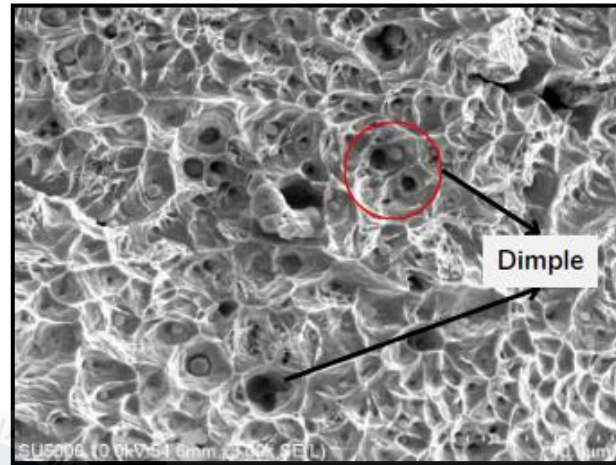


Figure 4.12: Microstructure fracture surface

The fractography depicted in the figure 4.12 illustrate of the tensile specimen provides vital insights into the failure process and material attributes. The specimen was examined using a Scanning Electron Microscope (SEM) using magnification of  $10\mu\text{m}$  reveals the presence of dimples, which indicate ductile fracture. Dimples occur when microvoids nucleate, grow, and merge, indicating that the material underwent considerable plastic deformation prior to collapse. The detected dimples in the fractography picture are numerous and evenly distributed, indicating a consistent ductile fracture throughout the material. This type of fracture is often desired in structural applications because it indicates that the material can absorb significant energy before failure, offering a warning through prolonged deformation. Direction specimens showed finer and deeper dimples. It was also observed that the diagonal specimens had shallower dimples, indicating that for the tensile specimen, the strength went in line with ductility similar fracture results were obtained by (Wu et al., 2018)

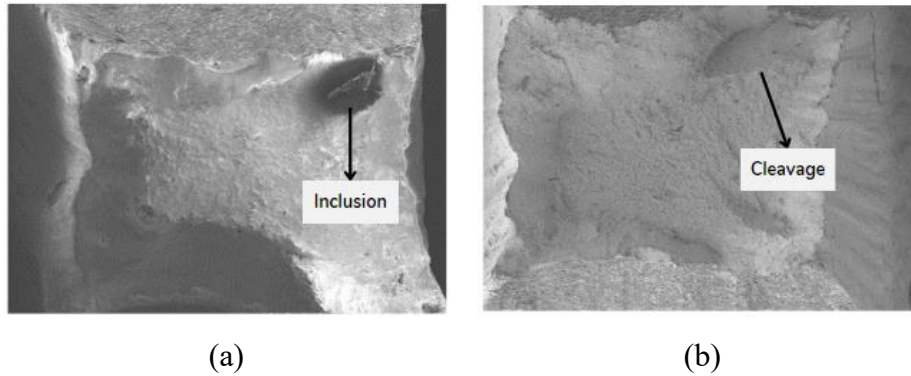


Figure 4.13: Fracture surface at (a) top surface, (b) bottom surface

Figure 4.13 shows the fracture surface of tensile specimen for 308 stainless steel. Image (a) reveals an inclusion, while image (b) indicates cleavage. These characteristics are critical for understanding the mechanical behaviour and failure processes of the material under tensile stress. Inclusions, as seen in image (a), are non-metallic particles or contaminants that are embedded in the metal matrix. These can come from a variety of sources, such as the base material, filler wire, or contamination during manufacture. The presence of an inclusion works as a stress concentrator, causing premature failure onset. Inclusions can drastically impair the material's ductility and toughness by providing sites for fracture formation and propagation during tensile stress. The inclusion in image (a) most likely contributed to localised stress concentration, which caused a crack to propagate, resulting in the observed fracture. Image (b) shows a cleavage fracture with flat, faceted surfaces. Cleavage is a brittle fracture mode in which the material breaks at specified crystallographic planes. This sort of fracture is common in materials with limited plastic deformation capabilities under circumstances, such as low temperatures or high strain rates. The presence of cleavage in 308 stainless steel indicates that the local stress conditions and probably the microstructure around the cleavage zone were favourable to brittle failure. Cleavage can be caused by excessive residual pressures from the WAAM process, inadequate post-processing heat treatment, or an intrinsically brittle microstructure in certain places.

## 4.7 Tensile Properties

The tensile properties of deposited 308 stainless steel were evaluated using 100KN tensile test machine, the table 4.3 shows the results of ultimate tensile strength, yield strength and elongation for 3 samples. the summarized data for 3 samples illustrate bar chart in figure 4.14 shows the differentiate result for each sample.

Table 4.3: Mechanical properties data

Sample	Ultimate tensile strength (MPa)	Yield strength (MPa)	Elongation (%)
Sample 1	565.799	452.344	69.84
Sample 2	562.153	424.913	78.1440
Sample 3	537.760	432.726	71.9760

Sample 1 had the highest ultimate tensile strength (UTS) at 565.799 MPa, followed by Sample 2 at 562.153 MPa and Sample 3 with the lowest at 537.760 MPa. Yield strength (YS) readings followed the same trend, with Sample 1 having the highest YS of 452.344 MPa, while Samples 2 and 3 had lower YS values of 424.913 MPa and 432.726 MPa, respectively. The elongation percentages varied substantially, with Sample 2 having the maximum ductility (78.144%), suggesting better plastic deformation capabilities before fracture. Sample 3 exhibited considerable elongation of 71.976%, whereas Sample 1 had the lowest at 69.84%.

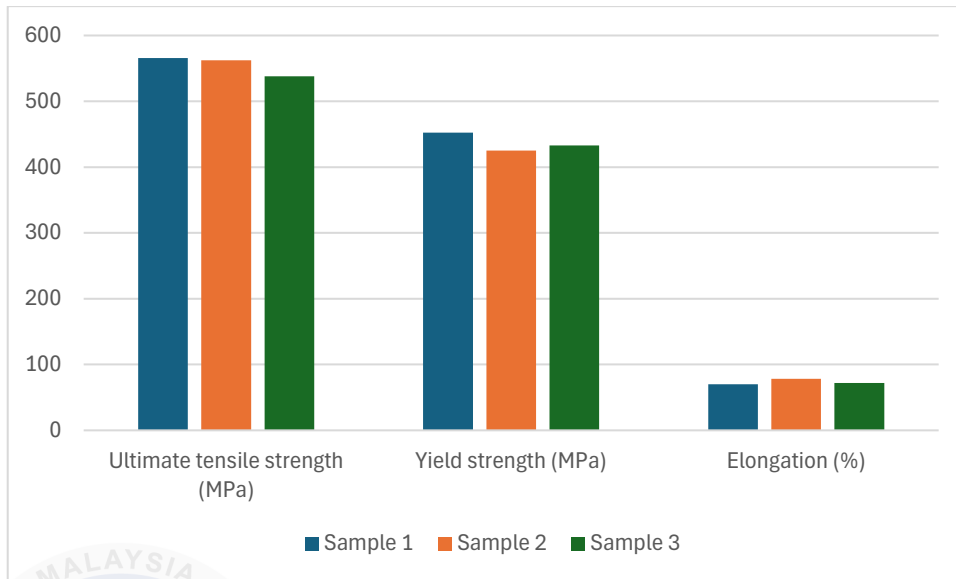


Figure 4.14: Comparison of the mechanical properties tensile test

Sample 1 has the highest tensile characteristics for high-strength applications, but Sample 2's greater elongation makes it appropriate for ductility-critical applications. Further microstructural investigation would offer further insight into the underlying causes of these disparities. These findings are consistent with prior research in the area that emphasise the necessity of optimised process parameters in obtaining desirable mechanical qualities in WAAM-produced stainless steel components. (Dash et al., 2023)

## 4.8 Effect of parameter on bead dimension

### 4.8.1 Analysis between parameter and width

The figure 4.15 below depicts a pareto chart showing the bead width effect. The chart below illustrates the relationship between the parameters and the width of the bead dimension. The parameters in this study are welding current, voltage, and welding speed. It was discovered that welding speed is the most significant level, followed by welding current, since the factor that crossed the reference line as marked in the chart below indicates that the

most significant influence on the width of the bead dimension. The welding speed has the biggest effect, resulting in a more substantial influence on the bead width dimension.

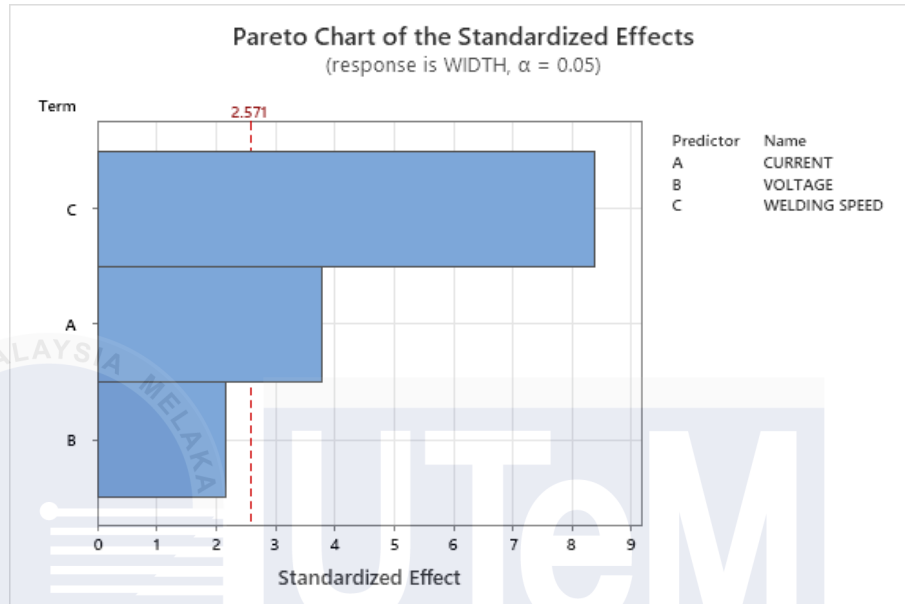


Figure 4.15: Pareto Chart of width effect

#### 4.8.2 Analysis between parameter and height

Figure 4.16 below depicts a pareto chart showing the bead height effect. The chart below depicts the relationship between the parameters and the height of the bead dimension. It was discovered that welding speed has the highest significant level, followed by welding current and voltage, because the factor that did not cross the reference line as marked in the chart below indicates that the significant factor on the height of the bead dimension has only a minor influence, but welding current has the greatest influence on the bead height. This welding speed has the most effect, resulting in a minor but considerable influence on the bead height dimension.



Figure 4.16: Pareto Chart of height effect

#### 4.9 Optimization of parameter

The optimization parameters seek for a combination of values that meets the requirements set for each response and factor. As a result, the highest parameter of optimization value was chosen as the preferred parameter value for each factor and response. The objective of this study is to determine the optimal value of wire arc additive manufacturing (WAAM) using GMAW process parameters for the bead dimension geometry. The Main Effects Plot for SN ratios for bead width in WAAM with GMAW for 308 stainless steel reveals how different factors influence bead width and height quality. The aim is to increase the signal-to-noise (SN) ratio, which indicates improved process stability and weld quality.

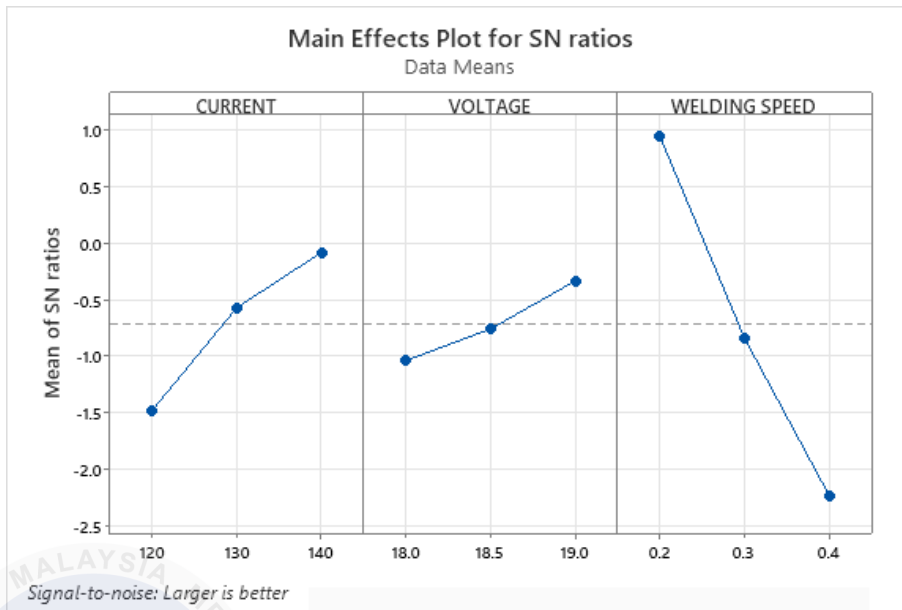


Figure 4.17: S/N ratio for width

The figure 4.17 depicts the optimization of parameters for the width bead effect. The parameters included welding current, voltage, and welding speed. This optimization SN ratio study was performed to determine the optimal value of each parameter influencing the width of the welding bead. To identify which value best indicates parameter optimization for width effects, the factor with the highest value for each factor was selected. The table 4.4 below shows the ideal value for each parameter and how it affects width bead.

Table 4.4: Optimization value for width effect

Welding Current (A)	Voltage (V)	Welding Speed (m/mm)
140	19	0.2

Figure 4.18 shows the optimization for the height effect. The parameters include weld current, voltage, and welding speed. The SN ratio graph shows the values used to determine the optimal value for each parameter regulating the height of the welding bead. To determine the optimum value for the height impact, inspect the highest value chart for each parameter factor. The table 4.5 shows the ideal value for each component that contributes to the height impact.

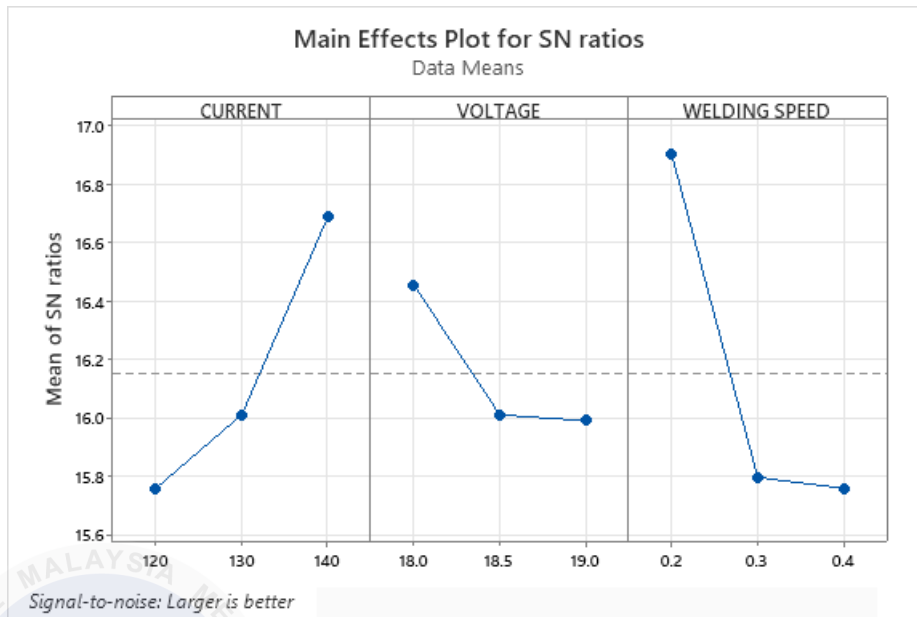


Figure 4.18: Pareto Chart for height

Table 4.5: Optimization value for height effect

Welding Current (A)	Voltage (V)	Welding Speed (m/mm)
140	18	0.2

For applications requiring massive metallic structures, bead width optimisation is essential because homogeneous bead dimensions guarantee uniform material deposition, maintain structural integrity, and lower the chance of flaws. Due to its influence on the precision of material deposition and structural integrity, bead width optimisation is essential in WAAM for large metallic structure application. Accurate bead measurements guarantee consistent stacking, mitigating flaws like as porosity and cracking, a crucial aspect of large-scale component performance and longevity. (Zhang et al., 2024) highlighted the importance of regulated bead width for structural applications, as it improves the overall quality and dependability of the deposited structures.

#### 4.10 Regression model

In this experiment, a regression model was created using Minitab software to determine the expected value of the experiment, as shown in the figure 4.19. The predicted outcome of the experiment was determined by substituting the optimization parameters into the regression equation for width weld bead, as illustrated below.

<b>Regression Equation</b> WIDTH = -1.235 + 0.00785 CURRENT + 0.0903 VOLTAGE - 1.738 WELDING SPEED
---

Figure 4.19: Regression equation for width

Predicted value =  $-1.235 + 0.00785 (140) + 0.0903 (19) - 1.738 (0.2)$   
= **1.2321 cm**

Next, the predicted value of the experiment as shows in figure 4.20 was obtained was to substitute the optimization parameters to the regression for height weld bead as shown below

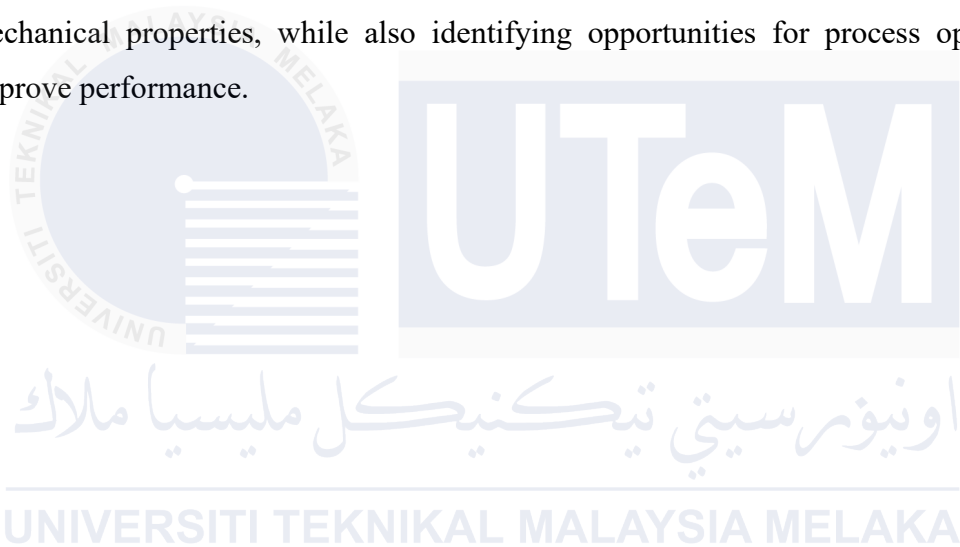
<b>Regression Equation</b> HEIGHT = 9.53 + 0.0333 CURRENT - 0.333 VOLTAGE - 4.17 WELDING SPEED
---

Figure 4.20: Regression equation for height

Predicted value =  $9.53 + 0.0333 (140) - 0.333 (18) - 4.17 (0.2)$   
= **7.364 mm**

## 4.11 Summary

This chapter summarises the results of the experiment. The microstructure and mechanical characteristics of 308 stainless steel were identified. The link between the parameters and the response was properly assessed and validated. The importance parameter, which influences the breadth and height of bead deposition, is also described. The optimal width and height characteristics were also observed. The study emphasises the potential of WAAM and GMAW in creating high-quality stainless steel components with acceptable mechanical properties, while also identifying opportunities for process optimisation to improve performance.



## **CHAPTER 5**

### **CONCLUSION AND RECOMENDATION**

#### **5.1 Conclusion**

This study successfully pinpointed the optimal Wire Arc Additive Manufacturing with GMAW process parameters of 308 stainless steel, which are crucial in determining the ideal process parameters for WAAM. The optimised parameters not only enable the production of high-performance 308 stainless steel components with WAAM but also enhance weld quality and process stability. For industrial applications where precise control over microstructure and mechanical characteristics is of utmost importance, the results offer practical suggestions. They also provide significant insights into the relationship between process factors and material qualities, underscoring the practical relevance of this research.

The samples generated with the optimised settings exhibited a refined grain structure with minimal defects, such as porosity and fractures, as confirmed by microstructural examination. The results of the tensile tests demonstrated that the optimised parameters produced a result that balanced tensile strength, with Sample 1 showing higher tensile strength (565.799 MPa). This successful achievement in determining the microstructure and mechanical properties of 308 stainless steel is a testament to the effectiveness of the research.

The findings show that bead height and width are most significantly influenced by welding speed, which is followed by welding current and voltage. The welding current of 140A, the voltage of 19V, and the welding speed of 0.2 m/min are the perfect parameters for producing the ideal bead width, according to the optimisation procedure. Similarly, for bead height, 18V for voltage, 140A for welding current, and 0.2 m/min for welding speed were

found to be the ideal values. The optimization of width bead been chosen due to the better application for large metallic structures. This successfully achieved the influence of effect parameters to bead geometry and optimization of bead geometry deposition.

## **5.2 Sustainable development**

In this regard, Wire Arc Additive Manufacturing applied in 308 stainless steel works toward the goals in terms of sustainable development through resource use efficiency and waste reduction. In this respect, WAAM can play a very essential role in industries that aim to reduce environmental impact since it enables the fabrication of complex structures with very low material wastage. Coupled with process parameter optimization, this project will be able to prove that WAAM can make quality components at a reduced energy consumption ratio if compared to traditional manufacturing methods. The optimization of welding current, voltage, and speed provides enhanced mechanical properties and process stability, thus lowering the risk of defects and rework. This efficiency ensures reduced resource consumption and a reduced carbon footprint, which is related to the sustainability agenda. Furthermore, this study can help industries embrace greener manufacturing practices and contribute towards sustainable industrial growth and the transition to greener manufacturing processes.

## **5.3 Complexity**

The complexity in the WAAM process optimization of 308 stainless steel lies in a multi-dimensional approach to achieving the right balance between diverse parameters to bring about the intended properties mechanically and microstructurally. In the light of this study, it was observed that the influence of welding current, welding voltage, and welding speed was intertwined but combined to affect bead geometry and material properties. It was observed that, under optimal conditions, microstructural analyses produced refined grains

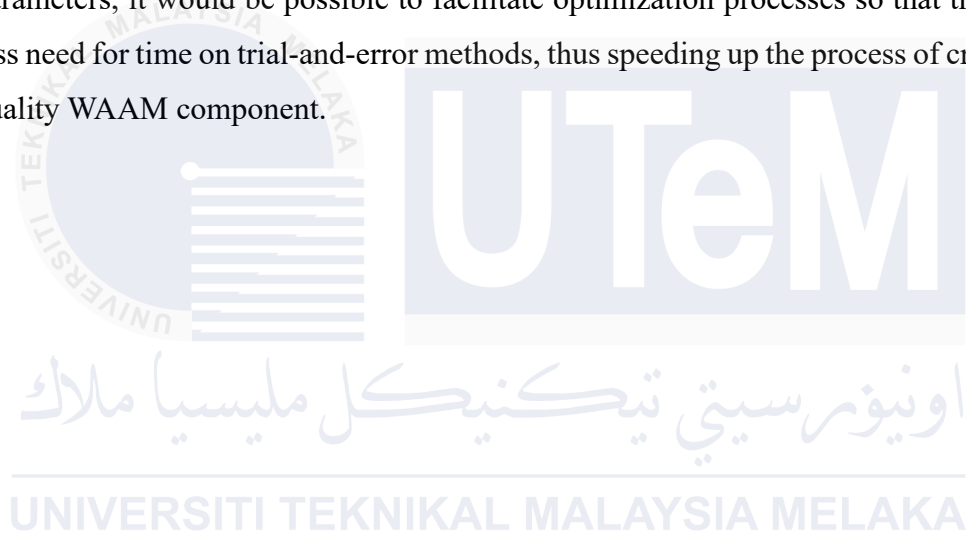
with minimal defects. The subtle effect of thermal cycles and solidification dynamics on the microstructure formation is very important. Capturing these complexities in experimental design required a robust experimental design coupled with a comprehensive analysis to isolate the effects of each parameter and understand them. This approach is so detailed that it immediately speaks to the requirement for accuracy in additive manufacturing processes—a small change may impart dramatic effects on the quality and performance of the end product. Therefore, results show that there is a need to refine and control WAAM processes to overcome inherent complexities and produce credible, high-quality output.

#### **5.4 Lifelong learning**

The one major requirement stressed by professionals from the engineering and manufacturing sectors working within this evolving field of WAAM is lifelong learning. The development of new technologies in this project meant it became a critical need to meet up with new technologies and process improvements realized. The continuous development and improvement of WAAM methodologies require practitioners to continuously educate and train themselves on mastering new tools and methodologies. This research work in process parameter optimization also exemplifies that theoretical knowledge alone cannot help solve practical and current manufacturing problems; rather, it needs to be supplemented by practical experience. Only this type of life-long learning can enable engineers and technicians to keep pace with fast-changing technologies, innovate in their domain of expertise, and adopt the best practices for improving productivity and sustainability. Consequently, the creation of a culture of continuous improvement and education is pivotal in remaining competitive and further developing the capabilities of additive manufacturing technologies.

## 5.5 Recommendations

Some recommendations based on the findings of this project could be put forward to further enhance the application of WAAM for 308 stainless steels. The parameters should be kept constant during the production process to obtain consistency for minimizing the generation of defects and increasing reliability. Regarding further research, the different shielding gases and wire composition that may influence WAAM processes need to be explored to broaden its versatility and scope of application. Finally, provided with sophisticated simulation tools for the prediction and analysis of the results of changes in parameters, it would be possible to facilitate optimization processes so that there would be less need for time on trial-and-error methods, thus speeding up the process of creating a high-quality WAAM component.



## REFERENCES

- Ajay, V., Nakrani, J., Mishra, N. K., & Shrivastava, A. (2023). Anisotropic fatigue crack propagation in wire arc additively manufactured 316L stainless steel. *International Journal of Fatigue*, 177. <https://doi.org/10.1016/j.ijfatigue.2023.107976>
- Ana Rosli, N., Rizal Alkahari, M., Redza Ramli, F., Nizam Sudin, M., & Maidin, S. (2020). Influence of Process Parameters in Wire and Arc Additive Manufacturing (WAAM) Process. *Journal of Mechanical Engineering*, 17(2), 69–78.
- Chaturvedi, M., Scutelnicu, E., Rusu, C. C., Mistodie, L. R., Mihailescu, D., & Arungalai Vendan, S. (2021). Wire arc additive manufacturing: Review on recent findings and challenges in industrial applications and materials characterization. In *Metals* (Vol. 11, Issue 6). MDPI AG. <https://doi.org/10.3390/met11060939>
- Chen, M. T., Gong, Z., Zhang, T., Zuo, W., Zhao, Y., Zhao, O., Zhang, G., & Wang, Z. (2024). Mechanical behavior of austenitic stainless steels produced by wire arc additive manufacturing. *Thin-Walled Structures*, 196. <https://doi.org/10.1016/j.tws.2023.111455>
- Chen, S., Xu, M., Yuan, T., Jiang, X., Zhang, H., & Zheng, X. (2022). Thermal–microstructural analysis of the mechanism of liquation cracks in wire-arc additive manufacturing of Al–Zn–Mg–Cu alloy. *Journal of Materials Research and Technology*, 16, 1260–1271. <https://doi.org/10.1016/j.jmrt.2021.12.016>
- Chen, X., Li, J., Cheng, X., He, B., Wang, H., & Huang, Z. (2017). Microstructure and mechanical properties of the austenitic stainless steel 316L fabricated by gas metal arc additive manufacturing. *Materials Science and Engineering: A*, 703, 567–577. <https://doi.org/10.1016/j.msea.2017.05.024>
- Cunningham, C. R., Flynn, J. M., Shokrani, A., Dhokia, V., & Newman, S. T. (2018). Invited review article: Strategies and processes for high quality wire arc additive manufacturing. In *Additive Manufacturing* (Vol. 22, pp. 672–686). Elsevier B.V. <https://doi.org/10.1016/j.addma.2018.06.020>
- Dash, A., Squires, L., Avila, J. D., Bose, S., & Bandyopadhyay, A. (2023). Influence of active cooling on microstructure and mechanical properties of wire arc additively

- manufactured mild steel. *Frontiers in Mechanical Engineering*, 9. <https://doi.org/10.3389/fmech.2023.1130407>
- Fang, X., Zhang, L., Li, H., Li, C., Huang, K., & Lu, B. (2018). Microstructure evolution and mechanical behavior of 2219 aluminum alloys additively fabricated by the cold metal transfer process. *Materials*, 11(5). <https://doi.org/10.3390/ma11050812>
- Hauser, T., Reisch, R. T., Breese, P. P., Lutz, B. S., Pantano, M., Nalam, Y., Bela, K., Kamps, T., Volpp, J., & Kaplan, A. F. H. (2021). Porosity in wire arc additive manufacturing of aluminium alloys. *Additive Manufacturing*, 41. <https://doi.org/10.1016/j.addma.2021.101993>
- Huang, X., Kwok, C. T., Niu, B., Luo, J., Zou, X., Cao, Y., Yi, J., Pan, L., Qiu, W., & Zhang, X. (2023). Anisotropic behavior of super duplex stainless steel fabricated by wire arc additive manufacturing. *Journal of Materials Research and Technology*, 27, 1651–1664. <https://doi.org/10.1016/j.jmrt.2023.10.005>
- Hussein, N. I. S., Mohd Jmmani, N. A. N., Ayof, M. N., Abd Rahim, T., Zainal Abidin, M. Z., Yusof, F., Jamaludin, M. F., & Williams, S. (2021). Simulation of wire and arc additive manufacturing of 308L stainless steel with cold arc gas metal arc welding. *Journal of Applied Engineering Design and Simulation*, 1(1), 88–96. <https://doi.org/10.24191/jaeds.v1i1.35>
- Jin, W., Zhang, C., Jin, S., Tian, Y., Wellmann, D., & Liu, W. (2020). Wire arc additive manufacturing of stainless steels: A review. In *Applied Sciences (Switzerland)* (Vol. 10, Issue 5). MDPI AG. <https://doi.org/10.3390/app10051563>
- Kumar, N., Bhavsar, H., Mahesh, P. V. S., Srivastava, A. K., Bora, B. J., Saxena, A., & Dixit, A. R. (2022). Wire Arc Additive Manufacturing – A revolutionary method in additive manufacturing. *Materials Chemistry and Physics*, 285. <https://doi.org/10.1016/j.matchemphys.2022.126144>
- Le, V. T., & Mai, D. S. (2020). Microstructural and mechanical characteristics of 308L stainless steel manufactured by gas metal arc welding-based additive manufacturing. *Materials Letters*, 271. <https://doi.org/10.1016/j.matlet.2020.127791>
- Le, V. T., Mai, D. S., Doan, T. K., & Paris, H. (2021a). Wire and arc additive manufacturing of 308L stainless steel components: Optimization of processing parameters and material

- properties. *Engineering Science and Technology, an International Journal*, 24(4), 1015–1026. <https://doi.org/10.1016/j.jestch.2021.01.009>
- Le, V. T., Mai, D. S., Doan, T. K., & Paris, H. (2021b). Wire and arc additive manufacturing of 308L stainless steel components: Optimization of processing parameters and material properties. *Engineering Science and Technology, an International Journal*, 24(4), 1015–1026. <https://doi.org/10.1016/j.jestch.2021.01.009>
- Lee, C., Seo, G., Kim, D., Kim, M., & Shin, J. H. (2021). Development of defect detection ai model for wire + arc additive manufacturing using high dynamic range images. *Applied Sciences (Switzerland)*, 11(16). <https://doi.org/10.3390/app11167541>
- Li, T., Wang, Z., Yang, Z., Shu, X., Xu, J., Wang, Y., & Hu, S. (2022). Fabrication and characterization of stainless steel 308 L / Inconel 625 functionally graded material with continuous change in composition by dual-wire arc additive manufacturing. *Journal of Alloys and Compounds*, 915. <https://doi.org/10.1016/j.jallcom.2022.165398>
- Li, Y., Luo, Y., Li, J., Song, D., Xu, B., & Chen, X. (2021). Ferrite formation and its effect on deformation mechanism of wire arc additive manufactured 308 L stainless steel. *Journal of Nuclear Materials*, 550. <https://doi.org/10.1016/j.jnucmat.2021.152933>
- Nagasai, B. P., Malarvizhi, S., & Balasubramanian, V. (2022). Mechanical properties and microstructural characteristics of wire arc additive manufactured 308 L stainless steel cylindrical components made by gas metal arc and cold metal transfer arc welding processes. *Journal of Materials Processing Technology*, 307. <https://doi.org/10.1016/j.jmatprotec.2022.117655>
- Palmeira Belotti, L., van Dommelen, J. A. W., Geers, M. G. D., Goulas, C., Ya, W., & Hoefnagels, J. P. M. (2022). Microstructural characterisation of thick-walled wire arc additively manufactured stainless steel. *Journal of Materials Processing Technology*, 299. <https://doi.org/10.1016/j.jmatprotec.2021.117373>
- Priarone, P. C., Pagone, E., Martina, F., Catalano, A. R., & Settineri, L. (2020). Multi-criteria environmental and economic impact assessment of wire arc additive manufacturing. *CIRP Annals*, 69(1), 37–40. <https://doi.org/10.1016/j.cirp.2020.04.010>
- Ren, D., Ba, X., Zhang, Z., Zhang, Z., Zhao, K., & Liu, L. (2023). Wire arc additive manufacturing of porous metal using welding pore defects. *Materials and Design*, 233. <https://doi.org/10.1016/j.matdes.2023.112213>

- Seow, C. E., Zhang, J., Coules, H. E., Wu, G., Jones, C., Ding, J., & Williams, S. (2020). Effect of crack-like defects on the fracture behaviour of Wire + Arc Additively Manufactured nickel-base Alloy 718. *Additive Manufacturing*, 36. <https://doi.org/10.1016/j.addma.2020.101578>
- Shukla, P., Chitral, S., Kumar, T., & Kiran, D. V. (2023). The influence of GMAW correction parameters on stabilizing the deposition characteristics for wire arc additive manufacturing. *Journal of Manufacturing Processes*, 90, 54–68. <https://doi.org/10.1016/j.jmapro.2023.01.075>
- Tomar, B., Shiva, S., & Nath, T. (2022). A review on wire arc additive manufacturing: Processing parameters, defects, quality improvement and recent advances. In *Materials Today Communications* (Vol. 31). Elsevier Ltd. <https://doi.org/10.1016/j.mtcomm.2022.103739>
- Vinoth, V., Sathiyamurthy, S., Natarajan, U., Venkatkumar, D., Prabhakaran, J., & Sanjeevi Prakash, K. (2022). Examination of microstructure properties of AISI 316L stainless steel fabricated by wire arc additive manufacturing. *Materials Today: Proceedings*, 66, 702–706. <https://doi.org/10.1016/j.matpr.2022.04.011>
- Vora, J., Parmar, H., Chaudhari, R., Khanna, S., Doshi, M., & Patel, V. (2022). Experimental investigations on mechanical properties of multi-layered structure fabricated by GMAW-based WAAM of SS316L. *Journal of Materials Research and Technology*, 20, 2748–2757. <https://doi.org/10.1016/j.jmrt.2022.08.074>
- Wang, Z., Palmer, T. A., & Beese, A. M. (2016). Effect of processing parameters on microstructure and tensile properties of austenitic stainless steel 304L made by directed energy deposition additive manufacturing. *Acta Materialia*, 110, 226–235. <https://doi.org/10.1016/j.actamat.2016.03.019>
- Wu, B., Pan, Z., Ding, D., Cuiuri, D., Li, H., Xu, J., & Norrish, J. (2018). A review of the wire arc additive manufacturing of metals: properties, defects and quality improvement. In *Journal of Manufacturing Processes* (Vol. 35, pp. 127–139). Elsevier Ltd. <https://doi.org/10.1016/j.jmapro.2018.08.001>
- Zhang, Z., Wang, Q., He, Y., Wang, X., Yuan, S., & Song, G. (2024). Microstructure and properties of multi-layer and multi-bead parts of 316 stainless steel fabricated by laser-

arc hybrid additive manufacturing. *Optics and Laser Technology*, 168.  
<https://doi.org/10.1016/j.optlastec.2023.109903>

Zhou, Y., Lin, X., Kang, N., Huang, W., Wang, J., & Wang, Z. (2020). Influence of travel speed on microstructure and mechanical properties of wire + arc additively manufactured 2219 aluminum alloy. *Journal of Materials Science and Technology*, 37, 143–153. <https://doi.org/10.1016/j.jmst.2019.06.016>



## APPENDIX A

Gantt chart of PSM 1

TASK	WEEK														
	1	2	3	4	5	6	7	8	9	10	11	12	13	14	15
PSM 1 Title Selection															
PSM 1 Title Conformation															
Discussion about the project with Supervisor															
Search for Relevant information of Journal and Articles															
Chapter 1 (Introduction)															
Chapter 2 (Literature Review)															
Chapter 3 (Methodology)															
References And Formatting															
Submission of Log Book to Supervisor															
Submission of General Conduct Form															
Poster Presentation															
Complete PSM 1 Report															
Final Report Submission															

Gantt Chart PSM 2

TASK	WEEK														
	1	2	3	4	5	6	7	8	9	10	11	12	13	14	15
PSM 2 Briefing	█														
References And Formatting		█													
Briefing by Laman Hikmah			█												
Lab progress			█	█	█	█	█	█	█	█	█	█	█	█	█
Chapter 4 (Result and Discussion)			█	█	█	█	█	█	█	█	█	█	█	█	█
English technical talk								█							
Technical report									█						
Submission of Log Book to Supervisor										█					
Project oral Presentation PSM 2											█				
Preparing Project report												█			
Project report submission to examiner													█		
Final report PSM 2 submission to supervisor														█	
CD submission of PSM 2 to faculty															█